The Pennsylvania State University

The Graduate School

Department of Physics

EVOLVING PARTICLE TRAJECTORIES PERTURBATIVELY AROUND ROTATING BLACK HOLES IN THE TIME DOMAIN

A Thesis in

Physics

by

Ramon Lopez-Aleman

Submitted in Partial Fulfillment
of the Requirements
for the Degree of

Doctor of Philosophy

August 2001

We approve the thesis of Ramon Lopez-Aleman.

Date of Signature

Jorge Pullin Professor of Physics Thesis Adviser Chair of Committee	
Pablo Laguna Professor of Astronomy and Astrophysics Co-Chair of Committee	
Abhay Ashtekar Eberly Professor of Physics	
Lee Samuel Finn Associate Professor of Physics and Astronomy and Astrophysics	
Jayanth Banavar Professor of Physics Head of the Department of Physics	

Abstract

Treating the Teukolsky perturbation equation numerically as a 2+1 PDE and smearing the singularities in the particle source term by the use of narrow gaussian distributions we have been able to reproduce earlier results for equatorial circular orbits and radial infall trajectories that were done using the more complex and computationally intensive frequency domain formalism using the Teukolsky or the Sasaki-Nakamura equations.

A time domain prescription for a more general evolution of circular orbits inclined with respect to the equatorial plane of the back hole simulating the orbital decay past the ISCO and the final plunge into the black hole will be presented. This approach can be extremely useful when tackling the more realistic problem of a compact star moving on a general orbit around a super-massive black hole under the influence of radiation reaction forces, since virtually all current prescriptions being considered to treat the radiation reaction forces include time-domain "tail-term" integrals over the past of the particle's worldline.

Table of Contents

List of Tables

List of Figures

Acknowledgments

I am most grateful and indebted to my thesis advisor, Jorge Pullin, for the encouragement he has shown me during my time here at Penn State, and for guiding me in my learning of General Relativity. I also thank profusely the Graduate School Fellowship Office and the Academic Computing Fellowship Program I was so lucky to be a part of. I am especially grateful for the financial and travel support which they have provided to me over the years. Many thanks also go to my friend and colleague, Gaurav Khanna, for helpful discussions and much needed help with the energy and angular momentum flux calculations. But most of all, I want to express my sincere appreciation to my wife Miriam and my whole family for their invaluable support and patience during the time this research was being conducted.

Preface

These are "interesting times" for relativists. We all hope that gravitational waves, one of the key predictions of Einstein's theory, will soon be unequivocally detected and will become one of the most valuable tools for observational astrophysics and cosmology. The ground-based interferometric detectors are now starting full-blown "science runs" and the plans for more sensitive second and even third generations are in the drawing boards. Even LISA, the space-based observatory seems to have a very good chance to obtain funding from ESA and NASA.

All these exciting experimental prospects for the near future drives the work of theorists to higher levels than in the "Golden Era" of black hole research in the '60s and '70s. Numerical relativity is rapidly coming of age and successfully grappling with many interesting problems on both the computational and fundamental physics arenas that promise many wonderful insights when solved.

This work tries to help in setting the stage for realistic calculations of what now seems to be a very likely occurrence in active galactic nuclei: the capture of compact stellar-sized white dwarfs or neutron stars by the supermassive black holes lurking in the center of most galaxies. This type of events will send strong bursts of gravitational waves right in LISA's planned sensitivity band.

Since the captured objects are small, they can be treated in a first approximation by the well established black hole perturbation theory. But one thorny problem still remains that has stalled progress in this area. We can model the waves coming from

many kinds of stationary particle orbits around the black hole, but real orbits will not be stationary. The emission of gravitational waves will kick back the object making the orbit decay in time. One of the challenges in this sub-field is to find workable prescriptions for these radiation reaction forces that can be used in numerical simulations that can produce accurate waveforms and energy fluxes for observers at large distances from the hole to be used as templates for the interferometric detectors. The prescriptions that have been worked out so far involve calculating quite complex integrals along the past light cone of the particle. Since almost all perturbative treatments of particles around rotating holes are done in the frequency domain, applying these radiation reaction schemes has been an impossible task.

We try here to work out a simple case of radiation reaction decay for circular adiabatic particle orbits around a rapidly rotating black hole to show how to treat this problem perturbatively in the time domain. We hope this might help to open the door to the use of these proposed fully relativistic radiation reaction schemes in the calculation of the more complex but interesting problem of modeling the orbital decay and gravitational radiation emission of particles in more general elliptic and/or inclined orbits.

Chapter 1

Introduction

The advent of the possibility of detecting gravitational waves with large interferometers (like the LIGO or VIRGO projects now in their final construction stages) is a very exciting prospect for relativists and astrophysicists. Besides being a formidable test of many of the most interesting predictions of Einstein's General Relativity in the poorly explored strong-field regime, gravitational wave astronomy holds the promise of a new and potentially rich way of looking at the universe in regions where electromagnetic radiation is usually trapped or scattered. The potential for new discoveries in areas like cosmology and galactic structure is inmense, but the experimental task of actually detecting gravitational wave strains of the order of 10^{-23} with ground-based interferometers is a very difficult one. The weakness of the predicted signals requires initial searches for very strong sources. The best theoretical candidates to date for detectable gravity wave sources are binary black hole collisions.

The evolution of a binary black hole system can be conceptually divided into three basic stages: (a) *inspiral*. At large enough separations the motion is relatively slow and the system proceeds thru many orbits in a slowly decaying inspiral movement due to emission of low level gravitational waves. This is analogous to what is observed in binary pulsars and can be well treated by Post-Newtonian approximation methods that try to match the motion and the energy fluxes as series expansion in the small parameter v/c.

(b) *plunge*. When the holes are close to each other and reach relativistic velocities, the system will pass thru the last stable orbit and the holes will plunge towards each other. In here there are no useful approximations, (other than treating the special case of one hole being much more smaller than the other), and each hole exerts a powerful non-linear influence on the spacetime around its neighbor and one must rely on numerical solutions of the full Einstein equations. The last phase is (c) the *ringdown* in which a common horizon envelops the merged holes which can be treated as a distorted single black hole and has been treated by perturbation methods[44] and in which the black holes rings down emitting gravitational radiation in a series of characteristic quasi-normal modes until it reaches a stationary state.

There is a very intense effort to numerically solve Einstein's equations in full non-linear form to provide accurate templates to aid in the detection of the waveform from such a collision. Due to the complexity of this task, this is a very ambitious problem still untractable even by state-of-the-art supercomputers. Full 3-D simulations using the ADM formalism[2] may not even be well-posed mathematically and suffer from multiple ambiguities due to difficulties in defining a proper gauge. They are memory intensive computations that at present can only follow the motion of the holes for only a short time, (in most cases less than a full orbit). This means that one needs astrophysically relevant initial data with which to start the simulation when the holes are really close to each other, and that is also a problem in which huge conceptual and computational difficulties prevent current progress.

Approximations like treating the last stages of the collision as a perturbation from a single stationary black hole spacetime or analyzing the case when one of the holes is

much more massive than the other using perturbation theory are very helpful both for aiding in the construction of a code for a full non-linear evolution and to shed light on the fundamental physics of the collision itself.

1.1 Perturbative Black Hole Methods

In black hole perturbation theory we want to linearize the Einstein equations for gravitational (and other matter fields) about one of the known stationary solutions that describe a black hole. This is a simplified procedure compared to the aim of full numerical relativity of solving the full non-linear set of equations, although the resulting equations can be quite messy in algebraic terms. In this way we can evolve small departures from the isolated black hole spacetime due to the presence of outside sources like particles, gravitational waves, or even collisions with other black holes (in the "close limit" where the two objects can be regarded as one distorted black hole). A very comprehensive treatment of black hole perturbation theory can be found in Chandrasekhar's classic textbook[10].

A straightforward way to do this is to consider metric perturbations. This is analogous to what is done in the linearized treatment of gravity when the metric is written as $g_{ab} = \eta_{ab} + h_{ab}$, where h_{ab} is small compared to the Minkowski metric. In the late 50's, Regge and Wheeler[47] were the first to do this by linearizing the vacuum Einstein equations about the Schwarzschild metric and using the symmetries inherent in the background metric to separate the angular and radial parts of the equation. They expand the solution in tensor spherical harmonics, leaving a rather simple Schrödinger-like equation to solve for the radial part of the odd-parity set of perturbations.

In 1970, Zerilli[60] managed to do a similar construction for the even-parity metric perturbations and obtained a second order equation on a single function of the first order metric deviations from the Schwarzschild background that contained all relevant information about gravitational radiation both at infinity and at the horizon. Both formalisms made use of a particular gauge choice known as the *Regge-Wheeler gauge*. If one wrote the metric perturbation functions in the Regge-Wheeler notation :

$$ds^2 = ds^2_{schw} + h_{\alpha\beta} dx^\alpha dx^\beta \tag{1.1}$$

The perturbations $h_{\alpha\beta}$, which describe the deviations from spherical symmetry, are expanded using Regge-Wheeler harmonics as

$$
\begin{aligned}
h_{tt} &= (1-2M/r)H_0^{(\ell m)}Y_{\ell m} && (1.2)\\
h_{tr} &= H_1^{(\ell m)}Y_{\ell m} && (1.3)\\
h_{t\theta} &= h_0^{(\ell m)}Y_{\ell m,\theta} - c_0^{(\ell m)}Y_{\ell m,\phi}/\sin\theta && (1.4)\\
h_{t\phi} &= h_0^{(\ell m)}Y_{\ell m,\phi} - c_0^{(\ell m)}\sin\theta Y_{\ell m,\theta} && (1.5)\\
h_{rr} &= (1-2M/r)^{-1}H_2^{(\ell m)}Y_{\ell m} && (1.6)\\
h_{r\theta} &= h_1^{(\ell m)}Y_{\ell m,\theta} - c_1^{(\ell m)}Y_{\ell m,\phi}/\sin\theta && (1.7)\\
h_{r\phi} &= h_1^{(\ell m)}Y_{\ell m,\phi} + c_1^{(\ell m)}\sin\theta Y_{\ell m,\theta} && (1.8)\\
h_{\theta\theta} &= r^2K^{(\ell m)}Y_{\ell m} + r^2G^{(\ell m)}Y_{\ell m,\theta\theta} \\
&\quad + c_2^{(\ell m)}(Y_{\ell m,\theta\phi} - \cot\theta Y_{\ell m,\phi})/\sin\theta && (1.9)\\
h_{\theta\phi} &= r^2G^{(\ell m)}\left(Y_{\ell m,\theta\phi} - \cot\theta Y_{\ell m,\phi}\right) \\
&\quad - c_2^{(\ell m)}\sin\theta(Y_{\ell m,\theta\theta} - \cot\theta Y_{\ell m,\theta} - Y_{\ell m}/\sin^2\theta)/2 && (1.10)\\
h_{\phi\phi} &= r^2K^{(\ell m)}\sin^2\theta Y_{\ell m} \\
&\quad + r^2G^{(\ell m)}\left(Y_{\ell m,\phi\phi} + \sin\theta\cos\theta Y_{\ell m,\theta}\right) \\
&\quad - c_2^{(\ell m)}\sin\theta(Y_{\ell m,\theta\phi} - \cot\theta Y_{\ell m,\phi}). && (1.11)
\end{aligned}
$$

In the Regge-Wheeler gauge choice, they can write a general gauge transformation such that the functions $G^{(\ell m)}$, $h_0^{(\ell m)}$, and $h_1^{(\ell m)}$ vanish, leaving only four unknown functions. This is done primarily for mathematical convenience.

The Regge-Wheeler metric approach, even when it has been quite useful for the Schwarzschild case, involves quite a lot of complex algebra, particularly when treating even-parity perturbations with the Zerilli equation. It is unfeasible to extend it to the more complex Kerr geometry. In addition, it suffers some of the same drawbacks as the linearized GR theory, since the perturbations are coordinate gauge dependent. If one does an infinitesimal coordinate translation $x_a \rightarrow x_a + \epsilon\xi_a$, the metric function h_{ab} transforms as

$$h_{ab} \rightarrow h_{ab} - 2\nabla_{(b}\,\xi_{a)} \tag{1.12}$$

The use of gauge dependent perturbations is warranted if one asks the right questions about global properties of the gravitational radiation and avoids trying to say anything about properties of the gravitational field at local events in the spacetime. Still one would be able to avoid all ambiguities if only gauge independent perturbations are considered. Moncrief[33] has devised a formalism closely related to the Zerilli one in which one can define a gauge independent waveform, but it does not appear to be applicable to the Kerr case.

The Kerr metric[21] is the axisymmetric solution to Einstein's field equations that describes the spacetime outside a stationary, rotating black hole. It is a type II-II in the Petrov classification scheme, which means that out of the four principal null directions that all stationary spacetimes can have it has two distinct principal null directions, (since the other two coincide with these).

These directions are null vectors that satisfy the following condition :

$$k^b k^c C_{abc[d}\, k_{e]} = 0 \tag{1.13}$$

where the C_{abcd} is the Weyl tensor.

This fact will be very convenient when treating curvature perturbations using the Newman-Penrose formalism[35] , since if one selects these principal null directions as the basis for the NP tetrad, one gets enough relations between the various spin coefficients to make the resulting system of equations easily solvable.

1.2 The Newman- Penrose formalism in GR

The Newman-Penrose formalism was developed to introduce spinor calculus into general relativity. It is a special instance of tetrad calculus[59]. Let us present a brief summary of the basic ideas behind the use of the formalism which will be used in deriving the Teukolsky equation.

One starts by introducing a complex null tetrad $\{\, \boldsymbol{l}, \boldsymbol{n}, \boldsymbol{m}, \boldsymbol{m}^* \,\}$ at each point in spacetime which consists of two real null vectors $\boldsymbol{l}, \boldsymbol{n}$ and one complex spacelike vector $\boldsymbol{m}$. These should satisfy the orthonormality relations

$$\boldsymbol{l} \cdot \boldsymbol{n} = \boldsymbol{m} \cdot \boldsymbol{m}^* = \mathbf{1} \tag{1.14}$$

with all other products being zero. Then $g_{ab} = -2[l_{(a} n_{b)} - m_{(a} m^*_{b)}]$. Now one defines four directional derivative operators along the tetrad directions

$$D = l^a \nabla_a, \qquad \Delta = n^a \nabla_a,$$
$$\delta = m^a \nabla_a, \qquad \delta^* = m^{*a} \nabla_a. \tag{1.15}$$

The basic quantities of the formalism are the *spin coefficients*, of which there are twelve complex ones :

$$\alpha = \tfrac{1}{2}\ (n^a m^{*b} \nabla_b l_a - m^{*a} m^{*b} \nabla_b m_a),$$
$$\beta = \tfrac{1}{2}\ (n^a m^b \nabla_b l_a - m^{*a} m^b \nabla_b m_a),$$
$$\gamma = \tfrac{1}{2}\ (n^a n^b \nabla_b l_a - m^{*a} n^b \nabla_b m_a),$$
$$\epsilon = \tfrac{1}{2}\ (n^a l^b \nabla_b l_a - m^a l^b \nabla_b m_a),$$
$$\lambda = -m^{*a} m^{*b} \nabla_b n_a, \quad \mu = -m^{*a} m^b \nabla_b n_a,$$
$$\nu = -m^{*a} n^b \nabla_b n_a, \quad \pi = -m^{*a} l^b \nabla_b n_a,$$
$$\kappa = m^a l^b \nabla_b l_a, \quad \rho = m^a m^{*b} \nabla_b l_a,$$
$$\sigma = m^a m^b \nabla_b l_a, \quad \tau = m^a n^b \nabla_b l_a \tag{1.16}$$

The whole set of field equations in the formalism come by writing the Ricci and Bianchi identities using these coefficients, and they take the place of the Einstein equations.

All ten independent components of the Weyl tensor can be written as five complex scalars:

$$\psi_0 = -C_{abcd}\, l^a m^b l^c m^d$$

$$\psi_1 = -C_{abcd}\, l^a n^b l^c m^d$$

$$\psi_2 = -\tfrac{1}{2}\, C_{abcd}(l^a m^b l^c m^d + l^a n^b m^c m^{*d})$$

$$\psi_3 = -C_{abcd}\, l^a n^b m^{*c} n^d$$

$$\psi_4 = -C_{abcd}\, n^a m^{*b} n^c m^{*d} \tag{1.17}$$

To do perturbation calculations one specifies the perturbed geometry by introducing slight changes in the tetrad like $\boldsymbol{l} = \boldsymbol{l^A} + \boldsymbol{l^B}, \boldsymbol{n} = \boldsymbol{n^A} + \boldsymbol{n^B}$, etc. Here the A terms are the unperturbed values and the B ones the small perturbation. Then, all the Newman-Penrose spin coefficients and other quantities can be also written in a similar fashion : $\psi_4 = \overset{A}{\psi_4} + \overset{B}{\psi_4}$, etc. The perturbation equations come from the Newman-Penrose set by keeping B terms only up to first order.

Chapter 2

The Teukolsky Equation

The Teukolsky equation is a powerful and very convenient way to deal with gauge invariant curvature perturbations of both the Kerr and Schwarzschild metrics, (in the latter case, it is known as the *Bardeen-Press* equation). It has a very nice, separable mathematical structure and is amenable to robust numerical integration. Many interesting results have been derived leading up to the ideal situation of using it to treat the close limit of a generic rotating black hole collision and the evolution of gravitational waveforms from it.

Up to now, basically all treatments have been based on the separability of the equation and calculate the energy and waveforms for the first few l multipoles of the spheroidal harmonics expansion once the radial part has been dealt with. However, for the purpose of detecting the gravitational waves from the inspiral collision of a binary black hole system using laser interferometers one would like to obtain the time integration of the full Teukolsky equation once we have started from reasonable initial data describing the two holes in close proximity to each other.

Krivan *et al.* [26] have devised a procedure to evolve perturbations in time from generic initial data using the Teukolsky equation. Their method analyzes the radiation at infinity by dealing with the $s = -2$ version of the equation. They avoid fully separating the Teukolsky function and use the ansatz

$$\psi \equiv e^{i\,m\phi} r^3 \Phi(t, r^*, \theta) \tag{2.1}$$

Then the equation is rewritten as a first order matrix equation and numerically integrated. It has given encouraging results in treating scalar fields, scattering of gravitational waves and analysis of quasi-normal ringing and power law tails of the outgoing radiation. This demonstrated the feasibility of this numerical approach for the homogeneous Teukolsky equation.

Let us now review how previous work on solving the Teukolsky Equation has been done and how these standard frequency domain methods compare with the newly developed time domain based ones.

2.1 Review of the Derivation in Boyer-Lindquist coordinates

In 1973, Teukolsky[58] used the Newman-Penrose formalism to the special case of the background geometry of a II-II type, (the Kerr or Schwarzschild black holes are both of this type). In this way he was able to deduce the linearized equations for full dynamical perturbations of the hole that could handle changes in its mass and angular momentum, interaction with accreting test matter or distant massive objects, etc.

This approach has many important advantages. First, it turns out rather surprisingly that the equations are separable, so that by Fourier transforming and expressing the solution as a series expansion of *spheroidal harmonics* one ends up with having to solve just an ordinary differential equation for the radial part just like in the Regge-Wheeler case (in fact, the solutions are related to each other by a transformation operator, as

we will discuss later). Second, since for gravitational perturbations the dependent variable will be constructed out of the Weyl tetrad components ψ_0 and ψ_4, this will describe *gauge independent* perturbations, because these are gauge-invariant quantities (for more details on how to determine the gauge dependence of perturbations in general, one can look up the review by Breuer[7]).

When one chooses the $\boldsymbol{l}$ and $\boldsymbol{n}$ vectors of the unperturbed tetrad along the repeated principal null directions of the Weyl tensor, then

$$\begin{aligned} \psi_0^A = \psi_1^A = \psi_3^A = \psi_4^A = 0 \\ \kappa^A = \sigma^A = \nu^A = \lambda^A = 0 \end{aligned} \tag{2.2}$$

By collecting from the Newman-Penrose equation set those that relate ψ_0, ψ_1 and ψ_2 with the spin coefficients and tetrad components of the stress-energy tensor, and linearizing about the perturbed values, Teukolsky gets (after some algebra) the following decoupled equation for the perturbed ψ_0 :

$$\begin{aligned} &[(D - 3\epsilon + \epsilon^* - 4\rho - \rho^*)(\Delta - 4\gamma + \mu) \\ &- (\delta + \pi^* - \alpha^* - 3\beta - 4\tau)(\delta^* + \pi - 4\alpha) - 3\psi_2]\psi_0^B = 4\pi T_0 \end{aligned} \tag{2.3}$$

where

$$T_{0} = (\delta + \pi^{*} - \alpha^{*} - 3\beta - 4\tau)[(D - 2\epsilon - 2\rho^{*})T^{B}_{lm} - (\delta + \pi^{*} - 2\alpha^{*} - 2\beta)T^{B}_{ll}] + (D - 3\epsilon + \epsilon^{*} - 4\rho - \rho^{*}) \times [(\delta + 2\pi^{*} - 2\beta)T^{B}_{lm} - (D + 2\epsilon + 2\epsilon^{*} - \rho^{*})T^{B}_{mm}] \tag{2.4}$$

Since the full set of NP equations remains invariant under the interchange $\boldsymbol{l} \leftrightarrow \boldsymbol{n}$, $\boldsymbol{m} \leftrightarrow \boldsymbol{m}^{*}$ (this is the basis of the related GHP method [48]), then by applying this transformation one can derive a similar equation for ψ^{B}_{4} :

$$[(\Delta + 3\gamma - \gamma^{*} + 4\mu + \mu^{*})(D + 4\epsilon - \rho) - (\delta^{*} - \tau^{*} + \beta^{*} + 3\alpha + 4\pi)(\delta - \tau + 4\beta) - 3\psi_{2}]\psi^{B}_{4} = 4\pi T_{4} \tag{2.5}$$

where

$$T_{4} = (\Delta + 3\gamma - \gamma^{*} + 4\mu + \mu^{*})[(\delta^{*} - 2\tau^{*} + 2\alpha)T^{B}_{nm^{*}} - (\Delta + 2\gamma - 2\gamma^{*} + \mu^{*})T^{B}_{m^{*}m^{*}}] + (\delta^{*} - \tau^{*} + \beta^{*} + 3\alpha + 4\pi) \times [(\Delta + 2\gamma + 2\mu^{*})T^{B}_{nm^{*}} - (\delta^{*} - \tau^{*} + 2\beta^{*} + 2\alpha)T^{B}_{nn}] \tag{2.6}$$

In a similar way, one can define tetrad components of the electromagnetic field tensor

$$\Phi_0 = F_{\mu\nu} l^\mu m^\nu, \quad \Phi_1 = \tfrac{1}{2}\, F_{\mu\nu}(l^\mu n^\nu + m^{*\mu} m^\nu), \quad \Phi_2 = F_{\mu\nu} m^{*\mu} n^\nu \tag{2.7}$$

and get similar decoupled equations for Φ_0 and Φ_2. One can try these ideas with neutrino and scalar fields also. So if one now writes the tetrads in Boyer-Lindquist [6] coordinates t, r, θ, ϕ (after using the gauge freedom these coordinates have to set up the spin coefficient $\epsilon = 0$) [23, 58] they become

$$l^\mu = [(r^2 + a^2)/\Delta, 1, 0, a/\Delta], \quad n^\mu = [r^2 + a^2, -\Delta, 0, a]/(2\Sigma),$$
$$m^\mu = [iasin\theta, 0, 1, i/sin\theta]/(\sqrt{2}(r + iacos\theta)) \tag{2.8}$$

where aM is the angular momentum of the black hole, $\Sigma = r^2 + a^2 cos^2\theta$, and $\Delta = r^2 - 2Mr + a^2$ (note that before one of the differential operators $n^\mu \partial_\mu$ was given the symbol Δ, but from now on it will have the more conventional sense described here). With these expressions one can now write explicitly the spin coefficients and ψ_2. Then it turns out that one can write all the decoupled equations for test scalar fields ($s = 0$), a test neutrino field ($s = \pm\frac{1}{2}$), a test electromagnetic field ($s = \pm 1$) or a gravitational perturbation ($s = \pm 2$) as a single master equation which is the famed *Teukolsky equation*:

$$\left[\frac{(r^2+a^2)^2}{\Delta}-a^2 sin^2\theta\right]\frac{\partial^2\psi}{\partial t^2}+\frac{4Mar}{\Delta}\frac{\partial^2\psi}{\partial t\partial\phi}+\left[\frac{a^2}{\Delta}-\frac{1}{sin^2\theta}\right]\frac{\partial^2\psi}{\partial\phi^2}$$
$$-\Delta^{-s}\frac{\partial}{\partial r}\left(\Delta^{s+1}\frac{\partial\psi}{\partial r}\right)-\frac{1}{sin\theta}\frac{\partial}{\partial\theta}\left(sin\theta\frac{\partial\psi}{\partial\theta}\right)-2s\left[\frac{a(r-M)}{\Delta}+\frac{i\,cos\theta}{sin^2\theta}\right]\frac{\partial\psi}{\partial\phi}$$
$$-2s\left[\frac{M(r^2-a^2)}{\Delta}-r-i\,a\,cos\theta\right]\frac{\partial\psi}{\partial t}+\left[s^2cot^2\theta-s\right]\psi=4\pi\Sigma T \tag{2.9}$$

For the case that interest us, which is where the perturbations are to be interpreted as gravitational radiation that can be measured at infinity, the value for $s=-2$, and in this case $\psi=\rho^{-4}\psi^{B}_{4}$, where $\rho=-1/(r-i\,a\,cos\theta)$ in the coordinates we are using, and $T=2\rho^{-4}T_{4}$.

As mentioned before, this equation turns out to be separable. If one writes the Teukolsky function as $\psi=e^{-i\,\omega t}e^{i\,m\phi}S(\theta)R(r)$ then the Teukolsky equation separates into a radial part and an angular part. The angular equation for $S(\theta)$ has as a complete set of eigenfunctions the "spin weighted spheroidal harmonics" [56] of weight s . The radial part has the general form

$$\left(\frac{d}{dr}p\frac{d}{dr}+p^2U\right)R=p^2T \tag{2.10}$$

In here, $p(r)=(r^2-2Mr)^{-1}$ and the effective potential is given by $U=(1-\frac{2M}{r})^{-1}[(\omega r)^2-4i\omega(r-3M)]-(l-1)(l+2)$, while T is the source term previously defined for $s=-2$. (This is for the simplified $a=0$ case. A slightly more complicated version

depending on the value of a for the fully rotating case can be found as equation (4.9) of Teukolsky [58].)

When the angular momentum a goes to zero, the Kerr metric goes to the Schwarzschild one and the Teukolsky equation becomes the Bardeen-Press equation. [4]

There is of course considerable interest in computing the energy carried off by outgoing waves at infinity due to the evolution of the perturbations from some initial data. The non-trivial information about outgoing waves at infinity is carried by the ψ_4^B tetrad component. In principle, it is possible to use the solution for ψ_4^B to solve the complete Newman-Penrose set of equations for the perturbations in the metric. So, for outgoing waves with frequency ω

$$\psi_4^B = -\omega^2 (h_{\theta\theta}^B - i\, h_{\theta\phi}^B)/2 \tag{2.11}$$

Therefore,

$$\frac{d^2E^{(out)}}{dtd\Omega} = \lim_{r\to\infty} \frac{r^2\omega^2}{16\pi}\left[(h_{\theta\theta}^B)^2 + (h_{\theta\phi}^B)^2\right] = \lim_{r\to\infty} \frac{r^2}{4\pi\omega^2} |\, \psi_4^B \,|^2 \tag{2.12}$$

2.2 Previous treatment of perturbations for orbiting particles

Both the Regge-Wheeler and the Teukolsky formalisms have been used extensively in one of the classical test cases for this perturbation calculations : that of a particle of mass $\mu \ll M$ falling into a stationary, isolated black hole. That can logically lead later on to extensions like considering the deformation and internal dynamics of an infalling

star, accretion disks [37] , and hopefully the late stages of a black hole collision in a not-too-distant future [44].

The first such calculation using a Green's function technique to integrate the recently derived Zerilli equation (the even-parity counterpart of the Regge-Wheeler equation) was done by Davis, Ruffini, Press and Price [13]. They computed for the first time the amount of energy that was given out as gravitational waves by a particle falling radially from infinity into a Schwarzschild black hole, and they found that it radiated $\Delta E = 0.0104\,\mu^2/M$ in geometrized units. The radiation from the $l = 2$ multipole dominates the spectrum and is peaked at $\omega = 0.32\ M^{-1}$, which is just a little below the fundamental resonant frequency for the black hole.

Sometime later, Ruffini [49] treated the case of a particle falling radially from infinity but with non-zero initial velocity, with the main result that the increase in radiated energy was minimal. More general treatments were attempted by Detweiler & Szedenits [15] which examined infall trajectories with nonzero angular momentum. Considerable increases in the emitted gravitational radiation are seen as the normalized angular momentum of the trajectory $J/\mu M$ increases from 0 to close to $4M$ (where the particle approaches a marginally bound, circular orbit). Increases in ΔE by a factor of 50 are found at the high J end.

The first calculation involving particles going into a Kerr black hole was carried out by Sasaki and Nakamura [52] who considered a particle falling radially along the symmetry axis of the hole. Several studies (all in the frequency domain) have been carried out dealing with infall in the equatorial plane (and the effect of the rotational frame dragging) [24], and with infall trajectories with finite angular momentum [25].

Quite a few detailed simulations of the gravitational waves emitted by a particle in a bound orbit around the black hole have also been carried out in recent years. The first results for radiation emitted by a particle in orbit around a Schwarzschild black hole were carried out by Detweiler, who was a pioneer in these techniques [14]. In a series of six papers, Poisson and various collaborators studied in detail using both analytic and numerical techniques the gravitational wave emission to infinity and into the horizon of a particle in circular orbit around a non-rotating hole [42, 39, 11, 41, 40, 1]. They used the Teukolsky equation in the frequency domain to do high accuracy numerical simulations of the orbiting particle as well as to calculate very high order Post-Newtonian corrections to the basic quadrupolar formula for the gravitational wave emission from the orbit.

Various researchers in Kyoto, Osaka and Waseda Universities in Japan have been doing extensive work on Post-Newtonian expansions for various types of particle orbits around Kerr holes based on a perturbative treatment as the exact relativistic model which motivates the various high order corrections [31]. They have worked on eccentric orbits around Schwarszchild[57], circular orbits slightly inclined away from the equatorial plane of Kerr holes[53], and particles with spin orbiting Kerr holes on equatorial circular orbits[55].

All this work has been done using a decomposition of the Teukolsky equation into spheroidal harmonics afforded by working in the frequency domain where the equation is fully separable. Let us briefly review exactly how this is done, and why from a strictly numerical point of view a switch in treating the Teukolsky equation in the *time domain* where it does not fully separate might be useful.

Authors	Type of result
Davis, Ruffini, Press & Price (1971)	radial infall from ∞ into Schwarzschild BH
Detweiler (1978) Poisson (1993,1995)	equatorial circular orbits around Kerr BH
Kojima & Nakamura (1984)	infall trajectories with ang mom $\neq 0$
Sasaki & Nakamura (1982)	infall along symmetry axis of Kerr BH
Tanaka *et al* (1996)	spinning particles in circ equatorial orbits
Hughes (1999)	slightly eccentric and non-equatorial orbits

Table 2.1. Some of the more relevant frequency domain results that have appeared in the recent literature.

2.3 Traditional Solution Method in the Frequency Domain

When the Teukolsky equation is fully separated one can write the ψ_4 independent variable as

$$\psi_4 = \frac{1}{r^4}\sum_{lm}\int d\omega e^{-i\omega t}\,{}_{-2}Y_{lm}(\theta,\varphi)\,R_{lm\omega}(r) \tag{2.13}$$

where ${}_{-2}Y_{lm}(\theta,\varphi)$ are the spheroidal harmonics of spin weight $s=-2$ which satisfy the angular equation

$$\frac{1}{\sin\theta}\frac{d}{d\theta}\left(\sin\theta\frac{d\,{}_sY^{a\omega}_{lm}}{d\theta}\right)+\Big[(a\omega)^2\cos^2\theta-2a\omega s\cos\theta$$
$$-\left(m^2+2ms\cos\theta+\frac{s^2}{\sin^2\theta}\right)+\mathcal{E}_{lm}\Big]\,{}_sY^{a\omega}_{lm}=0. \tag{2.14}$$

In here $\mathcal{E}_{lm}$ is the angular eigenvalue for which the equation has a solution ${}_sY^{a\omega}_{lm}$. The radial part of the Teukolsky equation is then given by

$$\Delta^2 \frac{d}{dr}\left(\frac{1}{\Delta}\frac{dR_{lm\omega}}{dr}\right) - V(r)\, R_{lm\omega} = T_{lm\omega} \tag{2.15}$$

in which the potential can be written as

$$V(r) = \frac{r^2}{\Delta}\left[\omega^2 r^2 - 4i\omega(r-3M)\right] - \lambda, \quad \Delta = r(r-2m), \tag{2.16}$$

and $\lambda = (l-1)(l+2)$ is the eigenvalue of the $s=-2$ spheroidal harmonics. The source term for this radial equation is constructed out of the stress-energy tensor in a somewhat similar fashion as we will detail later on for the time domain Teukolsky equation[31].

To solve Eq. (2.15), one constructs a Green function and the trick is to get the appropriate boundary conditions. As with all black hole spacetimes, the physically motivated boundary conditions consist on having waves purely ingoing at the horizon and purely outgoing at infinity. Then one only has to consider the following independent solutions of the homogeneous equation :

$$R^{\text{in}} \to \begin{cases} B^{\text{trans}}\Delta^2 e^{-i\omega r^*} & \text{for r} \to 2M, \\ r^3 B^{\text{ref}} e^{i\omega r^*} + r^{-1} B^{\text{inc}} e^{-i\omega r^*} & \text{for r} \to +\infty, \end{cases} \tag{2.17}$$

$$R^{\text{out}} \to \begin{cases} C^{\text{up}} e^{i\omega r^*} + \Delta^2 C^{\text{ref}} e^{-i\omega r^*} & \text{for r} \to 2M, \\ r^3 C^{\text{trans}} e^{i\omega r^*} & \text{for r} \to +\infty, \end{cases} \tag{2.18}$$

where r^* is the usual tortoise coordinate[47]. Then one can construct a solution as

$$R_{lm\omega} = \frac{1}{W}\left\{R^{\rm out}\int_{2M}^{r} dr'\,\frac{R^{\rm in}T_{lm\omega}}{\Delta} + R^{\rm in}\int_{r}^{\infty} dr'\,\frac{R^{\rm out}T_{lm\omega}}{\Delta}\right\} \tag{2.19}$$

in where the Wronskian is given by

$$W = \frac{1}{\Delta}\left[\left(\frac{d}{dr}R^{\rm out}\right)R^{\rm in} - R^{\rm out}\left(\frac{d}{dr}R^{\rm in}\right)\right] = 2i\omega C^{\rm trans}B^{\rm inc} \tag{2.20}$$

As one pushes the radius that one is interested on evaluating the function to extract gravitational wave information, the asymptotic behavior of the solution shows that

$$\begin{aligned} R_{lm\omega}(r\to\infty) &= \frac{r^3 e^{i\omega r^*}}{2i\omega B^{\rm inc}}\int_{2M}^{\infty} dr'\frac{T_{lm\omega}(r')R^{\rm in}(r')}{\Delta^2(r')} \\ &\equiv \tilde{Z}_{lm\omega} r^3 e^{i\omega r^*} \end{aligned} \tag{2.21}$$

The source term $T_{lm\omega}$ is constructed by an analogous process to that used to obtain Eq. (2.6) out of the stress energy tensor for a point particle

$$T^{\mu\nu} = \frac{\mu}{\Sigma\sin\theta dt/d\tau}\frac{dz^\mu}{d\tau}\frac{dz^\nu}{d\tau}\delta(r-r(t))\delta(\theta-\theta(t))\delta(\varphi-\varphi(t)) \tag{2.22}$$

The source term used in the Green Function construction will be given by

$$T_{lm\omega} = 4 \int \rho^{-5} \bar{\rho}^{-1} (B'_2 + B'^{*}_2) e^{-im\phi + i\omega t} {}_{-2}S^{a\omega}_{lm} d\Omega dt, \tag{2.23}$$

where

$$\begin{aligned} B'_2 &= -\frac{1}{2}\rho^8 \bar{\rho} L_{-1}[\rho^{-4} L_0(\rho^{-2}\bar{\rho}^{-1} T_{nn})] \\ &- \frac{1}{2\sqrt{2}}\rho^8 \bar{\rho}\Delta^2 L_{-1}[\rho^{-4}\bar{\rho}^2 J_+(\rho^{-2}\bar{\rho}^{-2}\Delta^{-1} T_{\bar{m}n})] \end{aligned} \tag{2.24}$$

$$\begin{aligned} B'^{*}_2 &= -\frac{1}{4}\rho^8 \bar{\rho} J_+[\rho^{-4} J_+(\rho^{-2}\bar{\rho} T_{\bar{m}\bar{m}}] \\ &- \frac{1}{2\sqrt{2}}\rho^8 \bar{\rho}\Delta^2 J_+[\rho^{-4}\bar{\rho}^2\Delta^{-1} L_{-1}(\rho^{-2}\bar{\rho}^{-2} T_{\bar{m}n})]. \end{aligned} \tag{2.25}$$

The operators L_s and J_+ are defined as

$$L_s = \partial_\theta + \frac{m}{\sin\theta} - a\omega\sin\theta + s\cot\theta \tag{2.26}$$

and

$$J_+ = \partial_r + i\frac{K}{\Delta}. \tag{2.27}$$

Since the radiation will be emitted at discrete harmonics of the orbital frequencies, one can see that

$$\tilde{Z}_{lm\omega} = Z_{lm} \sum_k \delta(\omega - \Omega_{mk}) \tag{2.28}$$

, in which the various compound harmonic frequencies $\Omega_{mk} = m\Omega_{\phi} + k\Omega_{\theta}$ are composed of the periods for θ and ϕ motions in the case of particle orbits around the massive hole. The connection of this solution with the gravitational radiation emitted by the perturbed system is encoded in the relation

$$\psi_4 = \frac{1}{2}(\ddot{h}_+ - i\ddot{h}_\times) \tag{2.29}$$

So that according to the expansion we did in Eq. (2.13)

$$h_+ - ih_\times = -\frac{2}{r}\sum_{lm}\int \frac{d\omega}{\omega^2}\tilde{Z}_{lm\omega}\ {}_{-2}Y_{lm}(\theta,\varphi)\, e^{-i\omega(t-r^*)} \tag{2.30}$$

And finally, in this commonly used formalism, the energy flux at infinity is given by

$$\left\langle \frac{dE}{dt} \right\rangle = \sum_{l=2}^{\infty}\sum_{m=1}^{l} \frac{|Z_{lm}|^2}{2\pi\omega_m^2} \tag{2.31}$$

If one is evaluating perturbations due to particles in orbit around a central black hole, to get good accuracies this procedure has to be done for values of l up to 12 for various harmonic frequencies, (more and more compound frequencies are involved for non-equatorial orbits as we will see later), requiring close to 3000 iterations on a rather complex numerical algorithm that involves all of the previously outlined steps and in some cases, quite more[19, 11].

2.4 Evolving the Teukolsky equation numerically in time

I will do all my work with the main numerical solutions provided by the latest version of a code originally developed by Laguna and collaborators[26] to evolve solutions of the Teukolsky equation in the time domain. In this case one will start with approximate initial data in a time slice provided by a point particle moving in orbit at a finite distance from the central large black hole. Although the techniques for dealing with the ψ_4 perturbations are more developed in the frequency domain, from a numerical point of view it is more feasible in this and other related cases to work in the time domain. Fourier transforming the initial data and performing the evolution with the separable equation for each frequency and transforming back the data on each desired time slice is more expensive than just evolving a more complex equation directly on the time domain. Mainly due to the fact that one would need a number of frequencies that is much greater than the number of angular components required to resolve the θ direction [26].

The Teukolsky code in the time domain rewrites the main equation (Eq. 2.9) as a couple of first order 2+1 partial differential equations for a main independent field proportional to the ψ_4 scalar and an auxiliary conjugate field.

The process starts by postulating an ansatz for the ψ function in Eq. (2.9) of the form

$$\psi = \Psi(r, t, \theta)\, e^{im\phi} \tag{2.32}$$

And to match this ϕ dependence, one would also want to write the source term as a similar Fourier decomposition

$$T = T_{m}(r,t,\theta)\, e^{im\phi} \tag{2.33}$$

For the sake of clarity in following the derivation of the evolution equation used in the code, let us rewrite here the main time domain Teukolsky equation :

$$\begin{aligned}
&\left[\frac{(r^2+a^2)^2}{\Delta} - a^2 sin^2\theta\right]\frac{\partial^2\psi}{\partial t^2} + \frac{4Mar}{\Delta}\frac{\partial^2\psi}{\partial t\partial\phi} + \left[\frac{a^2}{\Delta} - \frac{1}{sin^2\theta}\right]\frac{\partial^2\psi}{\partial\phi^2} \\
&-\Delta^{-s}\frac{\partial}{\partial r}\left(\Delta^{s+1}\frac{\partial\psi}{\partial r}\right) - \frac{1}{sin\theta}\frac{\partial}{\partial\theta}\left(sin\theta\frac{\partial\psi}{\partial\theta}\right) - 2s\left[\frac{a(r-M)}{\Delta} + \frac{i\,\cos\theta}{sin^2\theta}\right]\frac{\partial\psi}{\partial\phi} \\
&-2s\left[\frac{M(r^2-a^2)}{\Delta} - r - i\,a\,\cos\theta\right]\frac{\partial\psi}{\partial t} + \left[s^2 cot^2\theta - s\right]\psi = 4\pi\Sigma T
\end{aligned} \tag{2.34}$$

After eliminating the constant factors $e^{im\phi}$ and $1/\Delta$, and rearranging a little we have

$$\begin{aligned}
&-\left[(r^2+a^2)^2 - a^2\Delta sin^2\theta\right]\frac{\partial^2\Psi}{\partial t^2} \\
&-\left[4iMarm + 2s\left(r\Delta - M(r^2-a^2) + i\,a\,\Delta cos\theta\right)\right]\frac{\partial\Psi}{\partial t} \\
&+\Delta^{-s+1}\frac{\partial}{\partial r}\left(\Delta^{s+1}\frac{\partial\Psi}{\partial r}\right) + \frac{\Delta}{sin\theta}\frac{\partial}{\partial\theta}\left(sin\theta\frac{\partial\Psi}{\partial\theta}\right) \\
&+2sim\left[a(r-M) + \frac{i\,\Delta cos\theta}{sin^2\theta}\right]\Psi - \Delta\left[s^2 cot^2\theta - s\right]\Psi \\
&+m^2\left[a^2 - \frac{\Delta}{sin^2\theta}\right]\Psi = -4\pi\Sigma\Delta T_{m}
\end{aligned} \tag{2.35}$$

This can be simplified into

$$-\frac{\partial^2\Psi}{\partial t^2} - A\frac{\partial\Psi}{\partial t} + \frac{1}{\Sigma^*\Delta^{s-1}}\frac{\partial}{\partial r}\left(\Delta^{s+1}\frac{\partial\Psi}{\partial r}\right)$$
$$+\frac{\Delta}{\Sigma^* sin\theta}\frac{\partial}{\partial\theta}\left(sin\theta\frac{\partial\Psi}{\partial\theta}\right) - \tilde{V}\Psi = \frac{-4\pi\Sigma\Delta T_m}{\Sigma^*} \tag{2.36}$$

with the following term definitions:

$$\Sigma^* \equiv (r^2 + a^2)^2 - a^2\Delta sin^2\theta \tag{2.37}$$

$$A \equiv \frac{1}{\Sigma^*}\left[2s(r\Delta - M(r^2 - a^2)) + i\ (2sa\,\Delta cos\theta + 4Marm)\right] \tag{2.38}$$

$$\tilde{V} \equiv \frac{1}{\Sigma^*}\left(-2isma(r - M) + \frac{2sm\Delta cos\theta}{sin^2\theta}\right.$$
$$\left. + \Delta\left[s^2 cot^2\theta - s\right] + m^2\left[\frac{\Delta}{sin^2\theta} - a^2\right]\right) \tag{2.39}$$

One now switches from the radial Boyer-Lindquist coordinate to the Kerr tortoise coordinate[26] defined such that

$$\frac{\partial}{\partial r} = \frac{(r^2 + a^2)}{\Delta}\frac{\partial}{\partial r^*} \tag{2.40}$$

This will affect only the third term in Eq. (2.36). If one now proceeds by further decomposing the function Ψ into

$$\Psi(r,t,\theta) \equiv \frac{\Phi(r,t,\theta)}{f(r)},$$
$$f(r) \equiv \sqrt{\Delta^s(r^2+a^2)} \tag{2.41}$$

, then Eq, (2.36) becomes

$$-\frac{\partial^2\Psi}{\partial t^2} - A\frac{\partial\Psi}{\partial t} + \frac{(r^2+a^2)f}{\Sigma^*\Delta^s}\frac{\partial^2\Phi}{\partial r^{*2}} + \frac{\Delta}{\Sigma^* sin\theta}\frac{\partial}{\partial\theta}\left(sin\theta\frac{\partial\Psi}{\partial\theta}\right)$$
$$-\tilde{V}\Psi - \frac{(r^2+a^2)\Phi}{\Sigma^*\Delta^s}\frac{\partial^2 f}{\partial r^{*2}} = \frac{-4\pi\Sigma\Delta T_m}{\Sigma^*} \tag{2.42}$$

So, after a little algebraic manipulation we finally rewrite the Teukolsky equation in the form used in the evolution code:

$$-\frac{\partial^2\Phi}{\partial t^2} - A\frac{\partial\Phi}{\partial t} + b^2\frac{\partial^2\Phi}{\partial r^{*2}} + \frac{\Delta}{\Sigma^* sin\theta}\frac{\partial}{\partial\theta}\left(sin\theta\frac{\partial\Phi}{\partial\theta}\right) - V\Phi = \frac{-4\pi\Sigma\Delta f T_m}{\Sigma^*} \tag{2.43}$$

with

$$V \equiv \tilde{V} + \frac{f(r^2 + a^2)}{\Sigma^* \Delta^s} \frac{\partial^2 f}{\partial r^{*2}}$$

$$b \equiv \frac{(r^2 + a^2)}{\sqrt{\Sigma^*}}. \tag{2.44}$$

An auxiliary field Π is now introduced for the purpose of turning Eq. (2.43) into a set of two coupled first-order equations in space and time, chiefly because it will be more convenient to integrate it numerically using standard techniques.

$$\Pi = \frac{\partial \Phi}{\partial t} + b \frac{\partial \Phi}{\partial r^*} \tag{2.45}$$

$$\frac{\partial \Pi}{\partial t} + b \frac{\partial \Pi}{\partial r^*} = b(A - \frac{\partial b}{\partial r^*}) \frac{\partial \Phi}{\partial r^*} + \frac{\Delta}{\Sigma^* sin\theta} \frac{\partial}{\partial \theta} \left(sin\theta \frac{\partial \Phi}{\partial \theta} \right)$$
$$- A\,\Pi - V\Phi + \frac{4\pi \Sigma \Delta f\, T_m}{\Sigma^*} \tag{2.46}$$

This first order system is hyperbolic in the radial direction [26]. The system constituted by Eqs. (2.45) and (2.46) is discretized on a two dimensional polar grid. We work with a numerical code that produces very stable evolutions using a two-step Lax-Wendroff method [43]. The basic idea is to define a vector of all the components of the evolution field $\mathbf{u} = \{\Phi_R, \Phi_I, \Pi_R, \Pi_I\}$ and combine Eqs. (2.45) and (2.46) into a system of the form

$$\partial_t \mathbf{u} + \mathbf{D} \partial_{r^*} \mathbf{u} = \mathbf{S} \tag{2.47}$$

where one can write $\mathbf{D}$ as

$$\mathbf{D} = \begin{pmatrix} -b & 0 & 0 & 0 \\ 0 & -b & 0 & 0 \\ b(A_R - \frac{\partial b}{\partial r^*}) & -bA_I & -b & 0 \\ bA_I & b(A_R - \frac{\partial b}{\partial r^*}) & 0 & -b \end{pmatrix}$$

and $\mathbf{S}$ as

$$\mathbf{S} = \begin{pmatrix} \Pi_R \\ \Pi_I \\ \frac{\Delta}{\Sigma^* sin\theta}\frac{\partial}{\partial\theta}\left(sin\theta\frac{\partial\Phi_R}{\partial\theta}\right) - A_R\Pi_R + A_I\Pi_I - V_R\Phi_R + V_I\Phi_I + \frac{4\pi\Sigma\Delta f\, T_{mR}}{\Sigma^*} \\ \frac{\Delta}{\Sigma^* sin\theta}\frac{\partial}{\partial\theta}\left(sin\theta\frac{\partial\Phi_I}{\partial\theta}\right) - A_R\Pi_I - A_I\Pi_R - V_R\Phi_I - V_I\Phi_R + \frac{4\pi\Sigma\Delta f\, T_{mI}}{\Sigma^*} \end{pmatrix}$$

,and where A_R and A_I are the real and imaginary parts of the A coefficient defined above, and similarly for V_R, V_I, T_{mR} and T_{mI}.

In the first Lax-Wendroff step one defines half-grid intermediate values $\mathbf{u}^{n+1/2}_{i+1/2}$ by discretizing (2.47) like

$$\mathbf{u}^{n+1/2}_{i+1/2} = \frac{1}{2}\left(\mathbf{u}^{n}_{i+1} + \mathbf{u}^{n}_{i}\right) - \frac{\delta t}{2}\left[\frac{1}{\delta r^*}\mathbf{D}^{n}_{i+1/2}\left(\mathbf{u}^{n}_{i+1} - \mathbf{u}^{n}_{i}\right) - \mathbf{S}^{n}_{i+1/2}\right] \tag{2.48}$$

, where the angular indices have been omitted and are there in implicit form. All radial derivatives are taken by centered differences between values of i and $i+1$, and all

other algebraic terms in $\mathbf{D}^n_{i+1/2}$ and $\mathbf{S}^n_{i+1/2}$ are calculated by averaging over the values at i and $i+1$.

As in other applications of this Teukolsky code, we impose boundary conditions at the edges of the polar computational domain, i.e. at the black hole horizon, at the rotation axis and at the far end of the radial grid. The condition near the horizon is $\Phi = \Pi = 0$, due to the known asymptotic behavior of the fields[26, 58]. At the outer boundary we impose outgoing boundary conditions. These are not perfect and errors due to reflection from this boundary bounce back into the computational domain. We now deal with this by making the computational domain so large in the radial direction that any numerical reflections will not make it back to the point where we compute the waveforms and energy flux in the time allotted for the simulation. At the axis of rotation of the black hole one imposes the either the condition $\Phi = 0$ or $\partial_\theta \Phi = 0$ depending on the parity of the field specified by the azimuthal integer m. To avoid numerical instabilities at large values of m due to the nature of the real potential of the Teukolsky equation near the horizon, we also impose the secondary condition $\partial_{\theta,\theta}\Phi = 0$. We discuss in more detail the rationale behind our (admittedly bad) choice of initial data slice at the end of Section 3.2.

Grids typically used in this work with particle source terms are with $-50M \leq r^*_i \leq 400M$ and $0 \leq \theta_j \leq \pi$ with $i \simeq 4000$ and $j \simeq 20$.

Chapter 3

The Matter Source Term

3.1 Explicit General Form of the source

In Eq. (2.34), the source term T for the case in which $s = -2$ and the independent field is $\Psi = \rho^{-4}\psi_4$,(for which the Weyl scalar $\psi_4 = -C_{\alpha\beta\gamma\delta}n^{\alpha}m^{*\beta}n^{\gamma}m^{*\delta}$), will be given by $T = 2\rho^{-4}T_4$.

The T_4 expression was derived in Sec. (2.1), and its full expression is

$$\begin{aligned} T_4 &= (\Delta + 3\gamma - \gamma^* + 4\mu + \mu^*)[(\delta^* - 2\tau^* + 2\alpha)T_{nm^*} \\ &- (\Delta + 2\gamma - 2\gamma^* + \mu^*)T_{m^*m^*}] + (\delta^* - \tau^* + \beta^* + 3\alpha + 4\pi) \\ &\times[(\Delta + 2\gamma + 2\mu^*)T_{nm^*} - (\delta^* - \tau^* + 2\beta^* + 2\alpha)T_{nn}] \end{aligned} \tag{3.1}$$

In Boyer-Lindquist coordinates, with the use of the Kinnersley null tetrad[23] :

$$\begin{aligned} l^{\mu} = [(r^2 + a^2)/\Delta, 1, 0, a/\Delta], \quad n^{\mu} = [r^2 + a^2, -\Delta, 0, a]/(2\Sigma), \\ m^{\mu} = [iasin\theta, 0, 1, i/sin\theta]/(\sqrt{2}(r + iacos\theta)) \end{aligned} \tag{3.2}$$

, the relevant Newman-Penrose differential operators and spin coefficients are explicitly written in the following form

$$\Delta = n^{\mu}\partial_{\mu}$$

$$\delta^{*} = m^{*\mu}\partial_{\mu}$$

$$\rho = -\frac{1}{r - a\,i\,\cos(\theta)}$$

$$\tau = -\frac{a\,i\,\rho\,\rho^{*}\,\sin(\theta)}{\sqrt{2}}$$

$$\pi = \frac{a\,i\,\rho^{2}\,\sin(\theta)}{\sqrt{2}}$$

$$\beta = -\frac{\rho^{*}\,\cot(\theta)}{\sqrt{2}}$$

$$\alpha = \pi - \beta^{*}$$

$$\mu = \frac{\rho^{2}\,\rho^{*}\,\Delta}{2}$$

$$\gamma = \mu + \frac{\rho\,\rho^{*}\,(r - M)}{2} \tag{3.3}$$

The differential operators in the source term (3.1) will be expanded like

$$\Delta = \left((r^{2} + a^{2})\frac{\partial}{\partial t} - (r^{2} - 2Mr + a2)\frac{\partial}{\partial r} + a\frac{\partial}{\partial \phi}\right)/(2\Sigma)$$

$$\delta^{*} = \frac{1}{\sqrt{2}(r - ia\cos\theta)}(-ia\sin\theta\frac{\partial}{\partial t} + \frac{\partial}{\partial \theta} - i\csc\theta\frac{\partial}{\partial \phi}) \tag{3.4}$$

The complete source term after all terms in (3.1) are explicitly written in our chosen coordinate system and some algebra is carried out becomes

$$
\begin{aligned}
&T_{nn}\left(\left(\frac{(-r+i\,a\,\cos(\theta))\,\cot(\theta)+7\,i\,a\,\sin(\theta)}{\sqrt{2}\,(r-i\,a\,\cos(\theta))^2}-\tau\right)\left(\frac{-i\,\sqrt{2}\,a\,\sin(\theta)}{(r-i\,a\,\cos(\theta))^2}+\tau\right)\right.\\
&\left.-\frac{\frac{i\,\sqrt{2}\,a\,\cos(\theta)}{(r-i\,a\,\cos(\theta))^2}+\frac{2\,\sqrt{2}\,a^2\,\sin(\theta)^2}{(r-i\,a\,\cos(\theta))^3}-\partial_\theta\tau}{\sqrt{2}\,(r-i\,a\,\cos(\theta))}\right)+T_{mm}\left(\left(-\mu^*+\frac{2\,i\,a\,\cos(\theta)\,\Delta}{\Sigma^2}\right)\right.\\
&\left.\left(3\,\gamma-\gamma^*-\frac{(5\,r+3\,i\,a\,\cos(\theta))\,\Delta}{2\,\Sigma^2}\right)+\frac{\Delta\left(\frac{-2\,i\,a\,\cos(\theta)\,\Delta'}{\Sigma^2}+\partial_r\mu^*+\frac{4\,i\,a\,\cos(\theta)\,\Delta\,\partial_r\Sigma}{\Sigma^3}\right)}{2\,\Sigma}\right)+\\
&T_{nm}\left((2\,\alpha-2\,\tau)\left(3\,\gamma-\gamma^*-\frac{\Delta\,(5\,r+3\,i\,a\,\cos(\theta))}{2\,\Sigma^2}\right)+\left(2\,\gamma+2\,\mu^*\right)\right.\\
&\left.\left(-\tau+\frac{(-r+i\,a\,\cos(\theta))\,\cot(\theta)+7\,i\,a\,\sin(\theta)}{\sqrt{2}\,(r-i\,a\,\cos(\theta))^2}\right)+\frac{2\,\partial_\theta\gamma+2\,\partial_\theta\mu^*}{\sqrt{2}\,(r-i\,a\,\cos(\theta))}-\frac{\Delta\left(2\,\partial_r\alpha-2\,\partial_r\tau\right)}{2\,\Sigma}\right)+\\
&\partial_\phi(T_{mm})\left(\frac{-\left(a\left(\mu^*-\frac{2\,i\,a\,\Delta\,\cos(\theta)}{\Sigma^2}\right)\right)}{2\,\Sigma}-\frac{a\left(3\,\gamma-\gamma^*-\frac{\Delta\,(5\,r+3\,i\,a\,\cos(\theta))}{2\,\Sigma^2}\right)}{2\,\Sigma}-\frac{a\,\Delta\,\partial_r\Sigma}{4\,\Sigma^3}\right)+\\
&\partial_\phi(T_{nm})\left(-\frac{i\,\Delta\,\csc(\theta)}{2\sqrt{2}\,\Sigma\,(r-i\,a\,\cos(\theta))^2}+\frac{a\left(-\tau+\frac{(-r+i\,a\,\cos(\theta))\,\cot(\theta)+7\,i\,a\,\sin(\theta)}{\sqrt{2}\,(r-i\,a\,\cos(\theta))^2}\right)}{2\,\Sigma}-\right.\\
&\left.\frac{i\,\csc(\theta)\left(3\,\gamma-\frac{\Delta\,(5\,r+3\,i\,a\,\cos(\theta))}{2\,\Sigma^2}-\gamma^*+2\,\gamma+2\,\mu^*\right)}{\sqrt{2}\,(r-i\,a\,\cos(\theta))}-\frac{a\,\partial_\theta\Sigma}{2\,\sqrt{2}\,\Sigma^2\,(r-i\,a\,\cos(\theta))}+\frac{a\,(2\,\alpha-2\,\tau)}{2\,\Sigma}\right)+\\
&\partial_\phi(T_{nn})\left(\frac{i\,\csc(\theta)\left(-2\tau+\frac{(-r+i\,a\,\cos(\theta))\,\cot(\theta)+7\,i\,a\,\sin(\theta)}{\sqrt{2}\,(r-i\,a\,\cos(\theta))^2}+\frac{i\,\sqrt{2}\,a\,\sin(\theta)}{(r-i\,a\,\cos(\theta))^2}\right)}{\sqrt{2}\,(r-i\,a\,\cos(\theta))}+\right.\\
&\left.\frac{a-i\,r\,\cos(\theta)\,\cot(\theta)-a\,\cos(\theta)^2\,\cot(\theta)}{2\,(r-i\,a\,\cos(\theta))^3}\right)-\frac{a^2\,\partial_{\phi,\phi}(T_{mm})}{4\,\Sigma^2}-\frac{i\,a\,\csc(\theta)\,\partial_{\phi,\phi}(T_{nm})}{\sqrt{2}\,\Sigma\,(r-i\,a\,\cos(\theta))}+\frac{\csc(\theta)^2\,\partial_{\phi,\phi}(T_{nn})}{2\,(r-i\,a\,\cos(\theta))^2}+\\
&\partial_\theta(T_{nm})\left(\frac{\Delta}{2\,\sqrt{2}\,\Sigma\,(r-i\,a\,\cos(\theta))^2}+\frac{3\,\gamma-\frac{\Delta\,(5\,r+3\,i\,a\,\cos(\theta))}{2\,\Sigma^2}-\gamma^*}{\sqrt{2}\,(r-i\,a\,\cos(\theta))}+\frac{2\,\gamma+2\,\mu^*}{\sqrt{2}\,(r-i\,a\,\cos(\theta))}\right)+\\
&\partial_\theta(T_{nn})\left(\frac{2\,\sqrt{2}\,r^2\,\tau-2\,\sqrt{2}\,a^2\,\tau\cos(\theta)^2+r\,\cot(\theta)-8\,i\,a\,\sin(\theta)-i\,a\,\cot(\theta)\left(\cos(\theta)+4\,\sqrt{2}\,r\,\tau\,\sin(\theta)\right)}{2\,(r-i\,a\,\cos(\theta))^3}\right)+\\
&\frac{a\,\partial_{\theta,\phi}(T_{nm})}{\sqrt{2}\,\Sigma\,(r-i\,a\,\cos(\theta))}+\frac{i\,\csc(\theta)\,\partial_{\theta,\phi}(T_{nn})}{(r-i\,a\,\cos(\theta))^2}-\frac{\partial_{\theta,\theta}T_{nn}}{2\,(r-i\,a\,\cos(\theta))^2}+\\
&\partial_r(T_{mm})\left(\frac{-\Delta\left(5\,r\,\Delta-6\,\gamma\,\Sigma^2+7\,i\,a\,\Delta\,\cos(\theta)+2\,\Sigma^2\,\gamma^*-2\,\Sigma^2\,\mu^*\right)}{4\,\Sigma^3}+\frac{\Delta^2\,\partial_r\Sigma}{4\,\Sigma^3}-\frac{\Delta\,\Delta'}{4\,\Sigma^2}\right)+\\
&\partial_r(T_{nm})\left(-\frac{\Delta\,(\alpha-\tau)}{\Sigma}-\frac{\Delta\left(-\tau+\frac{(-r+i\,a\,\cos(\theta))\,\cot(\theta)+7\,i\,a\,\sin(\theta)}{\sqrt{2}\,(r-i\,a\,\cos(\theta))^2}\right)}{2\,\Sigma}+\frac{\Delta\,\partial_\theta\Sigma}{2\,\sqrt{2}\,\Sigma^2\,(r-i\,a\,\cos(\theta))}\right)+\\
&\frac{a\,\Delta\,\partial_{r,\phi}(T_{mm})}{2\,\Sigma^2}+\frac{i\,\Delta\,\csc(\theta)\,\partial_{r,\phi}(T_{nm})}{\sqrt{2}\,\Sigma\,(r-i\,a\,\cos(\theta))}-\frac{\Delta\,\partial_{r,\theta}(T_{nm})}{\sqrt{2}\,\Sigma\,(r-i\,a\,\cos(\theta))}-\frac{\Delta^2\,\partial_{r,r}(T_{mm})}{4\,\Sigma^2}+\\
&\partial_t(T_{mm})\left(\frac{\left(a^2+r^2\right)\left(5\,r\,\Delta-6\,\gamma\,\Sigma^2+7\,i\,a\,\Delta\,\cos(\theta)+2\,\Sigma^2\,\gamma^*-2\,\Sigma^2\,\mu^*-\Delta\,\partial_r\Sigma\right)}{4\,\Sigma^3}+\frac{r\,\Delta}{2\,\Sigma^2}\right)+\\
&\partial_t(T_{nm})\left(\frac{\left(a^2+r^2\right)\left(2\,(\alpha-\tau)-\tau+\frac{-((r-i\,a\,\cos(\theta))\,\cot(\theta))+7\,i\,a\,\sin(\theta)}{\sqrt{2}\,(r-i\,a\,\cos(\theta))^2}\right)}{2\,\Sigma}-\frac{\frac{i}{2}\,a\,\Delta\,\sin(\theta)}{\sqrt{2}\,\Sigma\,(r-i\,a\,\cos(\theta))^2}-\right.\\
&\left.\frac{\left(a^2+r^2\right)\partial_\theta\Sigma}{2\,\sqrt{2}\,\Sigma^2\,(r-i\,a\,\cos(\theta))}-\frac{a\,\sin(\theta)\left(-5\,r\,\Delta+2\,\gamma\,\Sigma^2-3\,i\,a\,\Delta\,\cos(\theta)-2\,\Sigma^2\,\gamma^*-4\,\Sigma^2\,\mu^*\right)}{2\,\sqrt{2}\,\Sigma^2\,(i\,r+a\,\cos(\theta))}\right)+\\
&\partial_t(T_{nn})\left(\frac{a\,(-i\,a+r\,\cos(\theta))}{2\,(i\,r+a\,\cos(\theta))^3}+\frac{i\,a\,\sin(\theta)}{\sqrt{2}\,(r-i\,a\,\cos(\theta))}\left(-2\,\tau+\frac{\cot(\theta)}{\sqrt{2}\,(-r+i\,a\,\cos(\theta))}+\frac{9\,i\,a\,\sin(\theta)}{\sqrt{2}\,(r-i\,a\,\cos(\theta))^2}\right)\right)-\\
&\frac{a\left(a^2+r^2\right)\partial_{t,\phi}(T_{mm})}{2\,\Sigma^2}+\partial_{t,\phi}(T_{nm})\left(\frac{-i\left(a^2+r^2\right)\csc(\theta)}{\sqrt{2}\,\Sigma\,(r-i\,a\,\cos(\theta))}-\frac{i\,a^2\,\sin(\theta)}{\sqrt{2}\,\Sigma\,(r-i\,a\,\cos(\theta))}\right)+\\
&\frac{a\,\partial_{t,\phi}(T_{nn})}{(r-i\,a\,\cos(\theta))^2}+\frac{\left(a^2+r^2\right)\partial_{t,\theta}(T_{nm})}{\sqrt{2}\,\Sigma\,(r-i\,a\,\cos(\theta))}+\frac{i\,a\,\sin(\theta)\,\partial_{t,\theta}(T_{nn})}{(r-i\,a\,\cos(\theta))^2}+\frac{\left(a^2+r^2\right)\Delta\,\partial_{t,r}(T_{mm})}{2\,\Sigma^2}+\\
&\frac{i\,a\,\Delta\,\sin(\theta)\,\partial_{t,r}(T_{nm})}{\sqrt{2}\,\Sigma\,(r-i\,a\,\cos(\theta))}-\frac{\left(a^2+r^2\right)^2\partial_{t,t}(T_{mm})}{4\,\Sigma^2}-\frac{i\,a\left(a^2+r^2\right)\sin(\theta)\,\partial_{t,t}(T_{nm})}{\sqrt{2}\,\Sigma\,(r-i\,a\,\cos(\theta))}+\frac{a^2\sin(\theta)^2\,\partial_{t,t}(T_{nn})}{2\,(r-i\,a\,\cos(\theta))^2}
\end{aligned}
\tag{3.5}
$$

, where for clarity the subscript m in the various tetrad contractions of the stress-energy tensor refers to contraction with the m^* complex vector.

In our simulations we consider a non-spinning point particle of mass μ moving in the exterior of a rotating Kerr black hole, for which the stress-energy tensor takes the form

$$T^{\mu\nu} = \frac{\mu}{\Sigma \sin(\theta)\, dt/d\tau} \frac{dz^\mu}{d\tau} \frac{dz^\nu}{d\tau} \delta(r - r(t))\delta(\theta - \theta(t))\delta(\phi - \phi(t)) \tag{3.6}$$

, where z^μ is taken to be a geodesic trajectory to first order and $\tau = \tau(t)$ is the proper time of the particle as it moves along that geodesic.

If one substitutes the explicit geodesic equations (4.6 - 4.9), (which we will discuss in more detail in the following section) in the previous expression for the particle stress-energy tensor and contract it with the appropriate full blown expressions for the null tetrad (3.2) we get that[31]

$$T_{nn} = \mu \frac{C_{nn}}{\sin\theta}\, \delta\left(r - r(t)\right) \delta\left(\theta - \theta(t)\right) \delta\left(\phi - \phi(t)\right), \tag{3.7}$$

$$T_{mn} = \mu \frac{C_{mn}}{\sin\theta}\, \delta\left(r - r(t)\right) \delta\left(\theta - \theta(t)\right) \delta\left(\phi - \phi(t)\right), \tag{3.8}$$

$$T_{mm} = \mu \frac{C_{mm}}{\sin\theta}\, \delta\left(r - r(t)\right) \delta\left(\theta - \theta(t)\right) \delta\left(\phi - \phi(t)\right), \tag{3.9}$$

where

$$C_{nn} = \frac{\left(E\left(a^2+r^2\right)+\Sigma\frac{dr}{d\tau}-a\,L_z\right)^2}{4\,\dot{t}\,\Sigma^3}, \tag{3.10}$$

$$C_{mn} = -\frac{\rho}{2\sqrt{2}\Sigma^2\dot{t}}\left(E(r^2+a^2)-aL_z+\Sigma\frac{dr}{d\tau}\right)\left(i\sin\theta(aE-\frac{L_z}{\sin^2\theta})\right), \tag{3.11}$$

$$C_{mm} = \frac{\rho^2}{2\Sigma\dot{t}}\left(i\sin\theta(aE-\frac{L_z}{\sin^2\theta})\right)^2 \tag{3.12}$$

and in which $\dot{t} = dt/d\tau$.

3.2 Specifying the particle trajectory on the computational grid (initial data issues)

In this thesis, I will concentrate on non-equatorial circular orbits as a test case to be used in all calculations since they offer the possibility of incorporating a so called "*poor man's radiation reaction*" approach pioneered by Hughes [19]. This is a simple and realistic approximation for specifying orbital decay due to emission of gravitational waves for this particular set of special orbits. The rest of this section and Section (4.2) in the following chapter discussing the implementation of radiation reaction in circular inclined orbits follow closely his approach to this topic. Since a circular orbit evolves to another circular orbit, we will then see that a prescription to calculate the change in the orbit's parameters can be consistently given to allow for evolving the orbit in time up to the innermost stable circular orbit (ISCO) in principle.

As we detailed at the end of section (2.4), we will have the code evolving the Teukolsky equation in a 2-D grid with typical resolutions of $0.1M$ per gridpoint in the

radial direction, and about 0.3 radians per gridpoint in the θ angular direction. From the full-blown expression we will code in the source subroutine, one can see, (for example, refer to Eqs. (3.10)-(3.12)), that in the time domain evolution the Dirac Delta functions remain as part of the source term even when they usually go out in the Fourier decomposition when one does the time integration. Since we do not go thru that step in this formalism, one must resort to some sort of approximation for handling the delta function in the numerical implementation, since it is unlikely to have the particle's position lying exactly on a point in the computational grid.

One option would have been to calculate the position of the particle in each timestep, and then perform an integration in a grid cell using "advanced time" ($v = t + r^*$) and "retarded time" ($u = t - r^*$) mixed coordinates, and then assign weighted average amounts of the source quantity so computed to each neighboring grid point depending on how close it was to the actual position of the particle according to the equations of motion[29]. For our purposes of trying to incorporate the effects of radiation reaction to the orbit of the particle as a function of time, this approach would not be convenient and would require heavy modifications to our geodesic integrators and to the prescription being used to calculate the effects of radiation reaction on circular orbits.

Since the beginning of this project, we opted for a different approximation used by other researchers[50] that consists of treating the position delta functions as very narrow gaussian distributions

$$\delta(x - x(t)) \approx \frac{1}{\sqrt{2\pi}\,\sigma} \exp\left(\frac{-(x - x(t))^2}{2\sigma^2}\right) \qquad \text{for } \sigma \text{ small.} \tag{3.13}$$

One must show that this substitution is appropriate by showing convergence of the obtained waveform as $\sigma \rightarrow 0$, and one must take special care in normalizing the mass correctly as the particle moves in the background Kerr spacetime so that integration over the whole gaussian density profile gives a constant mass throughout the whole trajectory.

Basically the criteria that the narrow gaussian approximation must satisfy while the particle moves thru a geodesic orbit is that $\int \delta^3(\vec{\mathbf{x}} - \vec{\mathbf{x}}(t))\sqrt{g^{(3)}}d^3x = 1$, where for the usual gaussian expression like that in (3.13) the 3-metric over which this property occurs is the 3-metric of flat-space. Therefore, to obtain a particle of constant mass μ as it moves in the background black hole spacetime we normalize the mass-density of the particle by the factor

$$N = \frac{\sqrt{\gamma^{(3)}}}{\sqrt{g^{(3)}}}, \tag{3.14}$$

where $\gamma^{(3)}$ is the 3-metric of flat space and $g^{(3)}$ is the 3-metric of a slice of constant Boyer-Lindquist time of the Kerr spacetime. We then normalize the particle mass as it moves thru the space by multiplying the quantity μ in the expressions (3.7) - (3.9) by this factor N.

The $\delta(\phi - \phi(t))$ function we handled analytically since the code only evolves the Teukolsky function Φ of Eq.(2.43) in 2 dimensions. Therefore in the code we made the following substitutions in each expanded term in Eq.(3.5)

$$\delta(\phi-\phi_{_p}) \;\rightarrow\; \frac{-1}{2\pi}\, e^{^{im\phi_{_p}}} \tag{3.15}$$

$$\partial_{_\phi}\,\delta(\phi-\phi_{_p}) \;\rightarrow\; \frac{-im}{2\pi}\, e^{^{im\phi_{_p}}} \tag{3.16}$$

$$\partial_{_{\phi,\phi}}\,\delta(\phi-\phi_{_p}) \;\rightarrow\; \frac{m^2}{2\pi}\, e^{^{im\phi_{_p}}} \tag{3.17}$$

,where $\phi_{_p}$ indicates the calculated ϕ coordinate of the particle for the timestep in which the source term is being computed according to the geodesic equation for the current circular orbit.

Another subtle computational issue in this approach is that in all terms of Eq.(3.5) we tacitly evaluate the source term dependence on r at the value $r_{_p}$, (the radius of the circular orbit in which the particle is at that time) instead of at the value of the Boyer-Lindquist radial coordinate in each point of the computational grid. As in Ref. [50], we have tried evaluating it both ways and for the accuracy level of our numerical evolutions the actual difference is negligible.

We also have to explain our handling of the initial data slice at which the evolution begins. In the simplest case possible, we started with a flat $\Phi = \Pi = 0$ set, which corresponds to a vacuum configuration with no orbiting particle in which the spacetime is just the stationary Kerr background. In the subsequent timesteps the non-homogeneous Teukolsky evolution is set into motion, with the source term being that of Eq.(3.5). This is like the particle appearing out of nowhere which produces an artificial burst of radiation flowing away from the starting location of the particle. If we specify a large enough grid in the radial direction such that in the time for this burst to reach the outer

boundary and bounce back to the location in which the waveforms, energies and angular momentum fluxes are being calculated, the particle can complete a few orbits, then we can get enough data to calculate what the next radius and inclination angle are after the effects of the radiation reaction prescription we are using are taken into account. Therefore, for periodic orbits the details of the initial data are not crucial and the errors introduced initially by a bad choice of initial data propagate away from the point where all relevant computations are taking place and only constrain the length of time available for the simulation of each member of the orbital decay sequence.

To get more realistic initial data slices, one could try constructing initial data sets that correctly satisfy the Hamiltonian and momentum constraints with prescriptions like that of Bowen and York[5] ,(which are of common use in numerical relativity circles), or modifications of particle limit data sets such as those of Lousto and Price[30]. These prescriptions specify the (γ_{ij}, K_{ij}) sets for use in standard ADM evolutions. To convert these quantities to the set $(\Phi, \delta_t \Phi)$ needed for the Teukolsky evolution, one can use the formulae developed in Ref.[9] developed for use with the close-limit formulation. We plan to explore in some future work the extent of the benefits that this more accurate prescriptions may bring to prolong the orbital simulations in the particle limit case in the near future.

Chapter 4

Implementation of Radiation Reaction Effects

4.1 Effects of radiation reaction in particle orbits

From the standpoint of LISA observations, we want to study the case of a relatively small compact object orbiting and slowly spiraling into a large supermassive black hole, like the ones people currently suspect to be lurking inside the nuclei of many galaxies.

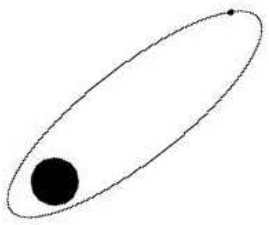

Fig. 4.1. Schematic diagram of a compact object orbiting a supermassive black hole.

In the case of general elliptical orbits the motion could be characterized by various characteristic orbital frequencies. First, the particle will cycle around the ellipse with

some frequency Ω_{ϕ}. Second, the ellipse will reside on a plane that passes thru the black hole, and the ellipse itself will rotate within the plane with some frequency Ω_{pp}. And finally, the plane itself will rotate around the spin axis of the hole with another frequency Ω_{S}. Various harmonics of these frequencies would be present in the gravitational wave emission coming from the system. As a first test of our time-domain perturbative approach we will restrict ourselves to circular orbits. Mainly to simplify the calculation, but there are also physical arguments to support this initial choice. Except for very eccentric elliptical orbits, one expects that gravitational wave emission would tend to circularize the orbit as the object spirals down from large distances.

Even objects that are small compared with the central black hole are unable to maintain stable circular orbits around it. One needs to specify how the particle spirals inward towards the hole due to loss of energy and angular momentum being radiated away by gravitational wave emission. Fortunately for most numerical simulations, in such a mass ratio limit the orbital decay is *adiabatic*. This means that the time scale for the particle to complete an orbit around the hole is much smaller than the time scale in which the parameters of the orbit change due to radiation reaction effects[19]. This is assuming all other external influences, like drag forces by accreting matter around the black hole are negligible. In most cases this appears to be true since astrophysicists believe that current evidence suggests that the majority of such disks develop via advection dominated accretion flow (ADAF)[34]. Basically, accretion disks of infalling matter around supermassive black holes are thought to be either thin or slim accretion disks for mass infall rates close to or above the Eddington rate, $\dot{M}_{Edd}$, or ADAF disks for non-active galactic nuclei. The majority of the suspected supermassive holes that live in

galactic nuclei should have ADAF accretion disks. In such thick ADAF disks, according to Narayan, drag related changes in the orbital phase will be of the order of 10^{-7} radians per year. This makes drag-related forces negligible and therefore a perturbative approach to gravitational radiation emission will be more than adequate to model such systems.

For the case that interests us, namely that of a few $M_{\odot}$ compact star orbiting in the strong field region of a $10^{6} M_{\odot}$ black hole, one can guess that the object will spend about a year spiraling from orbits with radii of about 4 M all the way to the ISCO. In that time, the gravitational waves will be sweeping the frequency band $7 \times 10^{-3}\text{Hz} \leq f \leq 3 \times 10^{-2}\text{Hz}$ which will pass right thru LISA's planned bandwidth of maximum sensitivity. The waves will be emitted for roughly 10^{5} cycles, which means that there will be ample opportunity to extract all the relevant system's parameters from them. According to the best current estimates[54] there may be enough of these systems to get about 1 event per year per GPc^{3} or even 1 per month, if we are lucky.

In a perturbative treatment, one can regard the motion of the particle as that of a geodesic in the background Kerr spacetime plus a small correction due to a time changing "radiation reaction force" $f^{\mu}_{RR}(\tau)$

$$\frac{dx^{\mu}}{d\tau} = \left.\frac{dx^{\mu}}{d\tau}\right|_{Kerr} + \int f^{\mu}_{RR}(\tau)\, d\tau \tag{4.1}$$

This force $f^{\mu}_{RR}(\tau)$ includes all effects of orbital decay due to emission of gravitational waves up to first order. We will see in Section 4.4 that accurate calculation of such forces imply evaluating integrals of the "tail" effects of scattering by the perturbation

along the past worldline of the particle. This suggests that the ability to evolve the waves in a time domain perturbative approach will be needed to tackle the problem of realistic orbital change due to radiation reaction forces.

Geodesic orbits around Kerr black holes can be parametrized by three constants of motion: $\mathbf{E}$, the energy; $\mathbf{L}_z$, the z-component of the angular momentum; and $\mathbf{Q}$, the Carter constant defined by $Q = p_\theta^2 + \cos^2\theta \left[a^2(1-E^2) + \csc^2\theta L_z^2\right]$. A specific (E, L_z, Q) set will be one point in the phase space of all possible Kerr orbits. So an orbit affected by radiation reaction will have a trajectory $(E(t), L_z(t), Q(t))$ on that phase space.

Let us now consider orbits as far from the horizon of the black hole as to be considered adiabatic. The change in orbital parameters from one orbit to the next will be nearly infinitesimal, and the particle will spend many orbits in practically the same point in the phase space of parameters. One can think of the decay as the passing of one geodesic orbit to another over the course of various revolutions. Of course, the closer the particle gets to the hole, the smaller the amount of revolutions one can regard the particle to spend in any specific geodesic orbit. Eventually, the decay will stop to be considered as adiabatic and one will need a full-nonlinear prescription for the equations of motion in the strong field region of the system. For circular or nearly-circular orbits, this plan of attack can take us all the way to the ISCO without seriously affecting the accuracy of the simulations.

This forms the basis of Scott Hughes' methodology for approximately treating the effects of radiation reaction in extreme mass ratio orbital binaries in the adiabatic limit

without actually having to calculate the radiation reaction force $f^{\mu}_{RR}(\tau)$[19]. This will be the main way in which we will implement radiation reaction in this work.

Basically, the idea is to attempt to read the changes in the parameter set (E, L_z, Q) out of the gravitational radiation flux at infinity, and then "move" the orbit to one characterized by

$$\begin{aligned} E_2 &= E_1 - \delta E \\ L_{z2} &= L_{z1} - \delta L_z \\ Q_2 &= Q_1 - \delta Q \end{aligned} \tag{4.2}$$

Sadly, this approach fails for most orbits. One can easily read changes in energy and angular momentum from the wave flux, but this is in most cases impossible for the change in the Carter Constant Q. The main reason for this difference is that the energy and angular momentum are quantities linearly constructed from the orbit's momentum p^{μ}, whereas the Carter Constant has a quadratic dependence on the momentum.

For a particle in a general orbit around a Kerr hole, it will have at any one instant a momentum p^{μ}_1. After many orbits, it will radiate away some momentum and later it can be considered to be in another quasi-equilibrium orbit, but now with momentum p^{μ}_2. We know that the Kerr metric admits a timelike Killing vector T_{μ}, an azimuthal Killing vector Φ_{μ}, and a Killing tensor $K_{\mu\nu}$[10].

So, for example, the energy of the orbiting particle will be given by $E = -T_{\mu}p^{\mu}$. Therefore the change in energy carried away by the radiation will be

$$\delta E = E_{2} - E_{1} = T_{\mu} p^{\mu} \tag{4.3}$$

This will depend only on the properties of the radiation extracted out at infinity or at the horizon, so this quantity, (and the angular momentum), can be extracted from the evolved ψ_{4} out of Teukolsky's equation.

In contrast, the Carter constant will be related to the orbital momentum as $Q = K_{\mu\nu} p^{\mu} p^{\nu}$. So if one writes the final momentum as $p^{\mu}_{2} = p^{\mu}_{1} + \delta p^{\mu}$ one can easily see that

$$\delta Q = Q_{2} - Q_{1} = 2K_{\mu\nu} p^{\mu} \delta p^{\nu} + K_{\mu\nu} \delta p^{\mu} \delta p^{\nu} \tag{4.4}$$

This quantity depends on the local instantaneous change of momentum and cannot in general be extract out of the emitted gravitational radiation. In fact, if one recognizes that in a suitable limit the quantity $\delta p^{\mu}/\delta\tau$ is the radiation reaction force, then one can see that

$$\dot{Q} = 2K_{\mu\nu} \delta p^{\mu} f^{\nu}_{RR} \tag{4.5}$$

So, in general one cannot escape the fact that one needs to calculate the local radiation reaction force acting on the orbiting particle to get to the next quasi-equilibrium orbit, even under the adiabatic regime. But there are 2 special cases in which this limitation can be overcome. One is the case of equatorial orbits, in which both Q and $\dot{Q}$ are zero. This is the easiest case to treat from the perturbative standpoint, and many precise results are available in the current literature [12, 11, 31, 39].

The second case, which we will analyze in this work, is that of circular (i.e., constant Boyer-Lindquist coordinate radius) non-equatorial orbits. Such orbits have a non-zero Carter Constant, but a powerful result proving that a circular orbit will remain circular as it decays [20, 51] makes them treatable without detailed knowledge of the radiation reaction force.

4.2 Radiation reaction treatment for circular orbits

Non-equatorial circular orbits have a non-zero Carter Constant. The object of this procedure is to establish the equilibrium values for the (E, L_z, Q) defining parameter set for such an orbit. Then using the fact that a circular orbit always evolves to another circular orbit one specifies the change in all three parameters from the gravitational radiation estimated by the numerical Teukolsky evolution.

The equations describing a geodesic $\frac{D\,u^\mu}{d\tau} = u^\nu\, u^\mu_{\ ;\nu} = 0$ in the Kerr spacetime are given by

$$\Sigma^2 \left(\frac{dr}{d\tau}\right)^2 = \left[E(r^2+a^2) - aL_z\right]^2 - \Delta\left[r^2 + (L_z - aE)^2 + Q\right] \equiv R\,, \quad (4.6)$$

$$\Sigma^2 \left(\frac{d\theta}{d\tau}\right)^2 = Q - \cot^2\theta L_z^2 - a^2\cos^2\theta(1-E^2)\,, \quad (4.7)$$

$$\Sigma\left(\frac{d\phi}{d\tau}\right) = \csc^2\theta L_z + aE\left(\frac{r^2+a^2}{\Delta} - 1\right) - \frac{a^2 L_z}{\Delta}\,, \quad (4.8)$$

$$\Sigma\left(\frac{dt}{d\tau}\right) = E\left[\frac{(r^2+a^2)^2}{\Delta} - a^2\sin^2\theta\right] + aL_z\left(1 - \frac{r^2+a^2}{\Delta}\right)\,. \quad (4.9)$$

in which E and L_z are the orbital energy and angular momentum component along the axis of rotation per unit mass of the particle, and Q is the Carter Constant for the orbit ($Q = Q^{total}/\mu^2$). A circular orbit satisfies $R = R' = 0$. These conditions specify that the radius must not change during the orbit and that the particle is always in a turning point of its radial motion. When one specifies r and L_z, then the conditions $R = R' = 0$ make possible the unambiguous determination of Q and E for that same orbit. These parameters specify a unique circular orbit whose inclination angle [51] will be given by

$$\cos\iota = \frac{L_z}{\sqrt{L^2{}_z + Q}}\,. \tag{4.10}$$

For orbits in the equatorial plane of the rotating hole, the inclination is $\iota = 0$ and $Q = 0$ for all times. Therefore the conditions $R = R' = 0$ can be used to solve for E and L_z as a function of the particle's radius.

$$E^p = \frac{1 - 2v + qv^3}{\sqrt{1 - 3v^2 + 2qv^3}}\,, \tag{4.11}$$

$$L^p_z = rv\frac{1 - 2qv^3 + q^2v^4}{\sqrt{1 - 3v^2 + 2qv^3}}\,, \tag{4.12}$$

$$E^r = \frac{1 - 2v - qv^3}{\sqrt{1 - 3v^2 - 2qv^3}}\,, \tag{4.13}$$

$$L^r_z = -rv\frac{1 + 2qv^3 + q^2v^4}{\sqrt{1 - 3v^2 - 2qv^3}} \tag{4.14}$$

E^p and L^p_z refer to prograde orbits with respect to the black hole spin, and E^r & L^r_z to the retrograde orbits. Here, $v \equiv \sqrt{M/r}$ and $q \equiv a/M$.

To treat non-equatorial circular orbits at some orbital radius r successfully one starts by noting that these orbits will have less angular momentum than the prograde equatorial orbit, which must be the most stable of them. Then the conditions $R = R' = 0$ allows one to get simple analytic expressions for $Q(r, L_z)$ and $E(r, L_z)$.

$$E(r, L_z) = \frac{a^2 L_z^2 (r - M) + r\Delta^2}{a L_z M(r^2 - a^2) \pm \Delta\sqrt{r^5(r - 3M) + a^4 r(r + M) + a^2 r^2 (L_z^2 - 2Mr + 2r^2)}}, \quad (4.15)$$

$$Q(r, L_z) = \frac{\left((a^2 + r^2)\, E(r, L_z) - a L_z\right)^2}{\Delta} - \left(r^2 + a^2 E(r, L_z)^2 - 2aE(r, L_z) L_z + L_z^2\right) \quad (4.16)$$

One can see that technically there are two roots for the orbital energy. In our work, we choose the plus sign in the denominator since the other sign usually gives energies which are less than the energy of the most strongly bound orbit (except on strong-field orbits of very rapidly rotating holes)[19]. Therefore, for the circular orbits of our interest, by fixing r and L_z one determines the orbit uniquely.

For inclined orbits around rotating holes, the period T_θ for spanning the inclination relative to the rotation axis (from θ_{min} to θ_{max} and back is different, and usually incommesurate, with the usual orbital period T_ϕ. This constitutes a problem for the frequency domain decompositions of the Teukolsky formalism since it is not entirely clear which frequency and its harmonics are the fundamental ones used in describing the orbits and the emitted gravitational radiation. It is customary[12, 19] to perform the

analysis in a particular frame of reference in which it can be shown that the ϕ motion can be Fourier expanded in the θ frequency harmonics.

The last and most important part of this scheme to approximate radiation reaction in our chosen orbits is to use the prescription of constant circularity to calculate the changes in the Carter Constant Q, the orbital radius and the inclination angle in an adiabatic manner. For an orbit to remain circular after decay the prescription is imposed that $\dot{R} = 0$ and $\dot{R'} = 0$, where again R is the right hand side expression of the radial geodesic equation (4.6). Specifically, we have

$$\begin{aligned}
\dot{R} &= \dot{r}R' + 2E\dot{E}r^4 + \left[2a^2E\dot{E} - 2L_z\dot{L_z} - \dot{Q}\right]r^2 + 2\left[\dot{Q}\right. \\
&\quad \left. +2(\dot{L_z} - a\dot{E})(L_z - aE)\right]Mr - a^2\dot{Q} = 0, \qquad (4.17) \\
\dot{R'} &= \dot{r}R'' + 8E\dot{E}r^3 + 2\left[2a^2E\dot{E} - 2L_z\dot{L_z} - \dot{Q}\right]r + 2\left[\dot{Q}\right. \\
&\quad \left. +2(\dot{L_z} - a\dot{E})(L_z - aE)\right]M = 0 \qquad (4.18)
\end{aligned}$$

From this set one can get a solution for $\dot{Q}$ and $\dot{r}$ in terms of the flux derived quantities $\dot{E}$ and $\dot{L_z}$. Thus, we may write

$$\begin{aligned}
\dot{Q} &= -\frac{c_{11}}{d}\dot{E} - \frac{c_{12}}{d}\dot{L}_z\,, \\
\dot{r} &= -\frac{c_{21}}{d}\dot{E} - \frac{c_{22}}{d}\dot{L}_z\,, \qquad (4.19)
\end{aligned}$$

where

$$
\begin{aligned}
c_{11}(Q,E,L_z,r) \equiv \quad & -4E(1-E^2)Mr^6 + 12EM^2r^5 - 2E[a^2(1-E^2)+3(L_z^2+Q)]Mr^4 \\
& +8[a^2E(2-E^2)+E(L_z^2+Q)-2aL_z]M^2r^3 \\
& -2a[aE[6M^2+L_z^2+Q+a^2(1-E^2)]-6M^2L_z]Mr^2 \\
& +4a^2E[Q+(L_z-aE)^2]M^2r - 4a(L_z-aE)[Q+(L_z-aE)^2]M^3 \ , \\
c_{12}(Q,E,L_z,r) \equiv \quad & -4L_z(1-E^2)Mr^4 + 16(1-E^2)(L_z-aE)M^2r^3 \\
& +2\left[L_z[a^2(1-E^2)+L_z^2+Q]-6M^2(L_z-aE)\right]Mr^2 \\
& -4L_z\left[Q+(L_z-aE)^2\right]M^2r + 4(L_z-aE)\left[Q+(L_z-aE)^2\right]M^3 \ , \\
c_{21}(Q,E,L_z,r) \equiv \quad & 2Er^5 - 6EMr^4 + 4a^2Er^3 + 2a(L_z-2aE)Mr^2 + 2a^4Er - 2a^3(L_z-aE)M \ , \\
c_{22}(Q,E,L_z,r) \equiv \quad & 2aEMr^2 - 2a^2L_zr + 2a^2(L_z-aE)M \ , \\
d(Q,E,L_z,r) \equiv \quad & -2(1-E^2)Mr^4 + 8(1-E^2)M^2r^3 + \left[Q+L_z^2-5a^2(1-E^2)-6M^2\right]Mr^2 \\
& +2\left[a^2(3-E^2)+2aEL_z-(L_z^2+Q)\right]M^2r \\
& +2(L_z^2+Q)M^3 - 4aEL_zM^3 + a^2(2E^2M^2-L_z^2-Q)M - a^4(1-E^2)M \ .
\end{aligned}
$$

By determining $\dot{E}$ and $\dot{L}_z$, we determine $\dot{Q}$ and $\dot{r}$, fully fixing the evolution of the particle's orbit. In particular, the rate of change of the inclination angle is

$$
\dot{\iota} = -\frac{d(\cos\iota)/dt}{1-\cos^2\iota} \ , \tag{4.20}
$$

where

$$
\frac{d(\cos\iota)}{dt} = \frac{1}{\sqrt{L_z^2+Q}}\left[\dot{L}_z - \left(\frac{L_z}{2}\right)\frac{2L_z\dot{L}_z+\dot{Q}}{L_z^2+Q}\right] \ . \tag{4.21}
$$

4.3 Numerical implementation of the circular orbit radiation reaction approximation

Our actual computational scheme involves (a) a Mathematica 3.0 notebook to compute the parameters that characterize the orbit, (b) a callable FORTRAN code to integrate the geodesic trajectory of the particle in the numerical 2-D grid (Boyer-Lindquist r and θ coordinates in the background Kerr spacetime) as well as the $e^{im\varphi}$ mode coefficients, (c) a FORTRAN routine to calculate the source term according to Eq.(3.5) at each timestep , (d) the main code to perform the numerical Teukolsky evolution in time; and finally, (e) another set of Mathematica tools to calculate how much energy and angular momentum has been radiated by the orbit and figure out by how much to alter the orbit parameters to get to next circular orbit in the sequence.

The geodesic integrator numerically integrates the Kerr geodesic equations (4.6 - 4.9) at each timestep and uses as input parameters the following quantities

1. r - the constant Boyer-Lindquist radius of the orbit.

2. σ_{r} and σ_{θ} - the radial and angular widths of the gaussian distributions which simulate the particle location in the computational domain. These are specified in terms of the number of gridcells that they will span.

3. L_{z} - the axial component of the angular momentum of the inclined circular orbit.

4. θ_{max} - the turning point of the θ coordinate of the orbit, (i.e. the maximum inclination angle of the orbit, which is closely related to the ι of Eq. (4.10) but is not exactly equal to it).

To specify initial data for a sequence of orbits one starts by choosing the starting radius and inclination angle one wants for the initial orbit. For that radial distance one calculates the value of L_z for the equatorial prograde orbit according to Eq. (4.12). This will be the upper bound value that L_z can attain for a circular orbit at that distance, and the actual value for an inclined orbit will be less than that. The Mathematica program implements a Newton-Rhapson search algorithm in the following manner: Start by reducing the value of L_z by an arbitrary set amount. Then calculate the values of E and Q according to equations (4.15) and (4.16). With the values of L_z and Q, use Eq. (4.10) to find the corresponding ι. Halve the difference ΔL_z used and apply to the new L_z value so as to approach the determined inclination angle one wants. Iterate this procedure until one gets within a tolerance of about $\epsilon \sim 10^{-7}$ of the starting value.

These results are fed to the source term subroutine which at each timestep of the evolution computes the source term using a discretization of Eq.(3.5) over the whole grid and solves the Teukolsky equation for the value of the ψ_4 field for at least 3 or more complete orbits. The programs monitors the value of ψ_4 at a set point in the grid far from the horizon and computes the energy and angular momentum fluxes in gravitational radiation according to the formulas[8, 22] :

$$\frac{\mathrm{d}E}{\mathrm{d}t} = \lim_{r\to\infty}\left\{\frac{1}{4\pi r^6}\int_\Omega \mathrm{d}\Omega \left|\int_{-\infty}^{t} \mathrm{d}\tilde{t}\,\psi_4(\tilde{t},r,\theta,\varphi)\right|^2\right\} \tag{4.22}$$

$$\begin{aligned}\frac{\mathrm{d}L_z}{\mathrm{d}t} = &-\lim_{r\to\infty}\left\{\frac{1}{4\pi r^6}\mathbf{Re}\left[\int_\Omega \mathrm{d}\Omega\left(\partial_\varphi\int_{-\infty}^{t}\mathrm{d}\tilde{t}\,\psi_4(\tilde{t},r,\theta,\varphi)\right)\right.\right.\\ &\left.\left.\times\left(\int_{-\infty}^{t}\mathrm{d}t'\int_{-\infty}^{t'}\mathrm{d}\tilde{t}\,\bar{\psi}_4(\tilde{t},r,\theta,\varphi)\right)\right]\right\} \qquad \mathrm{d}\Omega = \sin\theta\mathrm{d}\vartheta\mathrm{d}\varphi\end{aligned} \tag{4.23}$$

The code produces output files listing (a) the real and imaginary parts of the ψ_4 field at representative locations of the 2-D grid, and (b) the computed energy and angular momentum fluxes of Eqs.(4.22 - 4.23) for values of m from 1 to 8. And all this is done periodically at preselected times along the length of the simulation for a circular orbital geodesic.

The energy and angular momentum fluxes are averaged numerically over the time interval in which the particle completed as many orbits as the duration of the simulation allowed it. These fluxes are multiplied by the time it takes for 20-30 orbits and that energy and angular momentum change is used in a discretized version of Eq.(4.19) and (4.20) to get the corresponding changes in Q and ι due to the approximated effects of radiation reaction. With these new parameters we set up the next circular orbit on the sequence and in principle we can continue safely all the way down to the ISCO, although near it we should reduce the number of orbits used to calculate the parameter changes to maintain a similar level of accuracy. This method has the capacity to maintain as high a calculational precision as one needs by increasing the resolution of the grid and devoting more computer resources to the task. In this dissertation we do not intend to achieve the same level of precision as those of Ref. [11] and [18], but only to demonstrate the feasibility of this method to tackle the problem of radiation reaction in perturbative orbits, since as we will see in the next section almost all current proposals to understand and calculate the actual radiation reaction forces need to integrate in time along the past light cone of the particle.

4.4 More general prescriptions to calculate reaction forces for a particle

Using the preceding computational schemes one can approximate the effects of radiation reaction by energy balance considerations for equatorial or circular orbits only, so those are the only cases we have tackled in our research project. This severe limitation has been encountered by all studies of particle motion around black holes[18] since to treat more general orbital trajectories one would need a workable expression for $\dot{Q}$ and as we have just seen in Eq./,(4.5) one must know the local radiation reaction force f^{μ}_{RR} to get it.

In recent years this problem has interested many researchers and quite a few proposals have been presented for understanding and trying to define rigorously the leading order correction to the equation of motion of a particle moving in a geodesic of a background vacuum black hole spacetime. One proposal of Mino *et al* [32] involves a curved spacetime generalization of the well-known formalism of DeWitt and Brehme [16] to treat the electromagnetic self-force of an electrically charged particle. In the straightforward point particle limit this has unsurmountable conceptual difficulties as the stress-energy tensor of both the electromagnetic and gravitational fields becomes singular and therefore any other matter fields comprising the body must also become singular in order to "hold the particle together". So a sensible point particle limit in which the size of the body goes to zero while maintaining the charge and the mass of the body does not exist. What Mino *et al* propose is the construction of a conserved rank two symmetric tensor that will be integrated inside the interior of a world tube surrounding

the orbit. This tensor will encode the stress-energy of the matter field and a carefully defined trace reversed metric perturbation due to the presence of the particle on top of the background hole metric. Integrations of the tensor divergence over the top and bottom of an infinitesimal length of the tube give the definition of the particle momenta at both ends and the difference between them will be the change of momentum during that interval. This has to be equated to the momentum flow given by the integration of the tensor divergence over the surface of the tube. That is the basis of obtaining the equation of motion.

This result is not entirely rigorous since a crucial step in obtaining the final result is the use of an ansatz based on the assumption that in the point particle limit the momentum is always proportional to the 4-velocity of the particle. In the electromagnetic case where one can consider the extended charge distribution of the body to be supported by another force which will not be affected by the self-field of the particle and there will be no distortions in this distribution due to the radiation reaction this is justified, but one cannot be sure of this for the gravitational case.

The main equation of motion in this proposal looks like

$$\begin{aligned} m\ddot{z}_{\alpha}(\tau) &= -m\left(\frac{1}{2}\dot{z}_{\alpha}\dot{z}^{\beta}\dot{z}_{\gamma}\dot{z}^{\delta} + g^{\alpha\beta}\dot{z}_{\gamma}\dot{z}^{\delta} - \frac{1}{2}g^{\alpha\delta}\dot{z}^{\beta}\dot{z}_{\gamma}\right. \\ &\quad \left. -\frac{1}{4}g^{\beta\gamma}\dot{z}^{\alpha}\dot{z}^{\delta} - \frac{1}{4} - \frac{1}{4}g^{\alpha\delta}g^{\beta\gamma}\right)(\tau)\psi_{(\upsilon)\beta\gamma;\delta}(z(\tau)) \end{aligned} \tag{4.24}$$

where basically the quantity $\psi_{(\upsilon)\beta\gamma;\delta}(z(\tau))$ is the "tail-term" part of the trace reversed metric perturbation mentioned earlier. This has an unknown function defined

in term of the Green function of the linearized Einstein equation. This fact and the inherent difficulties of computationally implementing this tail-term integrations in the past section of the particle worldline in a generalized gauge choice is what has precluded the use of these formulas in actual studies of inclined and/or eccentric particle orbits around rotating black holes.

Quinn and Wald [45, 46] have also analyzed the problem of radiation reaction in a particle by postulating an axiomatic approach that tries to regularize the Green function of the linearized Einstein equation at the level in which the perturbed metric due to the particle enters at first order. They introduce a "comparison axiom" that more or less states that if two particles of the same mass m have the same four-acceleration on different spacetimes then the difference of their gravitational forces can be found by an effective integral expression averaged over a small sphere around the point in their worldlines where the comparison is made. This eliminates the singular part of the self-field of the particle and can be manipulated to give equations of motion that appear to agree substantially with those of Mino *et al.*

The main point here is that even when there are still doubts about energy conservation and questions of rigor in the derivation of the linearized equations of motion, these approaches would need to calculate the radiation reaction forces by performing "tail-term" integrations in the past worldline of the particle. So in the strong-field region a method to evolve the path of the particle in time as it orbit decays would be the ideal setting in which to finally implement these prescriptions in a numerically feasible way.

Chapter 5

Numerical Results

5.1 Reproduction of earlier frequency-based results

The main purpose of this research is to provide an alternative method to handle particle orbits around rotating black holes. This will be done in a novel way by providing a good approximation to the matter source term in the Teukolsky formalism in a way that could be used in the future as a practical means of providing for numerical implementations of tail-term integrals needed in most prescriptions of general radiation reaction forces for such orbits.

Since equatorial orbits have been treated with great precision in the frequency domain method, it is important to show that our method gives comparable results if one looks at quantities like the average gravitational energy flux at large distances from the horizon. Finn and Thorne [18] recently published a comprehensive work that tabulates and includes all previous results for high-precision gravitational wave flux and wave amplitudes coming from many kinds of representative compact objects in equatorial circular orbits around massive central black holes that LISA might detect with confidence. In Table 5.1 we make representative comparisons with the results of formulas (3.8) and (3.10) of that paper using the precise relativistic corrections included in Tables III - VI that they also provide.

We can see that there is substantial agreement with those results after we average the calculated energy flux using Eq. (4.22) at a grid point located at $r = 100M$ and $\theta = \pi$, which as a good an approximation to infinity as we are going to get in this algorithm. We have verified that small changes in model parameters like the width of the gaussian distribution, changing the location where the Teukolsky wave is measured, or the resolution of the grid do not change the results appreciably. The values computed in Table 5.1 with our code represent the optimum value for such parameters.

For the case of inclined orbits we compare the averaged energy flux output of our code with the content of Figures (4) and (9) of Hughes' paper[19] for the fiducial case of $r = 7M$, spin angular momentum $a = 0.95$ and $\iota = 62.43^{\circ}$. The results are in good semi-quantitative agreement since the exact values are not published in that paper and one has to sum over the values of $\frac{dE}{dt}$ for a few relevant values of the angular decomposition numbers l and m and our result comes from averaging the flux in time for one direction in space.

5.2 Convergence issues

We used the case of equatorial orbits around a non-rotating hole to verify the validity of our basic approach since there are many precise studies of the resulting waveforms and radiated energy fluxes emitted in this case, both numerically and analytically.[39, 19, 11, 31] It is also much easier to construct the source term since most of the terms in Eq. (3.5) vanish for such a case and an earlier, smaller version of the code ran much faster to do these kinds of tests. We also verified using computer algebra and a few experiments

Parameters	**Mode**	**Ratio between Finn-Thorne flux and our average flux**
$a = 0.9$, $r = 1.4\, r_{isco}$	$m = 2$	12.7007
	$m = 3$	2.96379
$a = 0.9$, $r = 3\, r_{isco}$	$m = 2$	2.10242
	$m = 3$	0.918952
$a = 0.9$, $r = 5\, r_{isco}$	$m = 2$	0.70204
	$m = 3$	0.299905
$a = 0.9$, $r = 6\, r_{isco}$	$m = 2$	0.522219
	$m = 3$	0.215364
$a = 0.5$, $r = 1.4\, r_{isco}$	$m = 2$	11.3851
	$m = 3$	4.93138
$a = 0.5$, $r = 2.5\, r_{isco}$	$m = 2$	2.67986
	$m = 3$	1.16467
$a = 0.5$, $r = 3\, r_{isco}$	$m = 2$	1.91827
	$m = 3$	0.808455
$a = 0.5$, $r = 5\, r_{isco}$	$m = 2$	1.51198
	$m = 3$	0.517028
$a = 0.5$, $r = 6\, r_{isco}$	$m = 2$	0.699328
	$m = 3$	0.228741

Table 5.1. Comparisons of gravitational wave energy fluxes detected at infinity using the frequency domain solution of the Teukolsky-Sasaki-Nakamura equation $\dot{E}_{\infty m}$ as calculated in Ref.[18] with the results measured numerically using the implementation of Eq. (4.22) at $r = 100M$ while evolving the Teukolsky equation in the time domain under the "particle-as -a-gaussian-distribution" approximation discussed here.

that the full version of the code agreed with this leaner version for the equatorial orbits around Schwarzschild cases.

Our approach was to compare the average energy flux emitted after a few orbits (without imposing changes due to radiation reaction) with the very precise average energy flux tables calculated by numerically integrating the Teukolsky equation in the frequency domain that appear in Ref.[11], and seeing how well does our evolution matches it as we make $\sigma \to 0$ up to the point where the code is still able to adequately resolve both the gaussian and its first two spatial derivatives. The gaussians and their derivatives used in Eq. (3.5) are calculated analytically in the code, and it is found that gaussian widths σ of a relative size as small as 0.8 gridpoints produce a source term that can be adequately resolved by the discrete grid used in the simulation.

The shape of Figure 5.1 indicate that for very small widths of the gaussian, the approximation of replacing a Delta function by a narrow gaussian peak seems to hold as expected. Therefore the results are independent of the actual width of the gaussian distribution used in the calculation.

For other evolutions in inclined circular orbits to demonstrate the use of the technique to follow a particle as the orbit decays under radiation reaction we used this minimum value of $\sigma/\Delta x = 0.8$, which we have verified that still provides adequate resolution of the gaussian (and its first two derivatives) on the computational grid.

We also made standard convergence tests by assuming that the numerical values included errors that decrease as a power of the grid spacing h. Specifically we assume that the value of the Teukolsky function Ψ at any point in the computational domain goes like

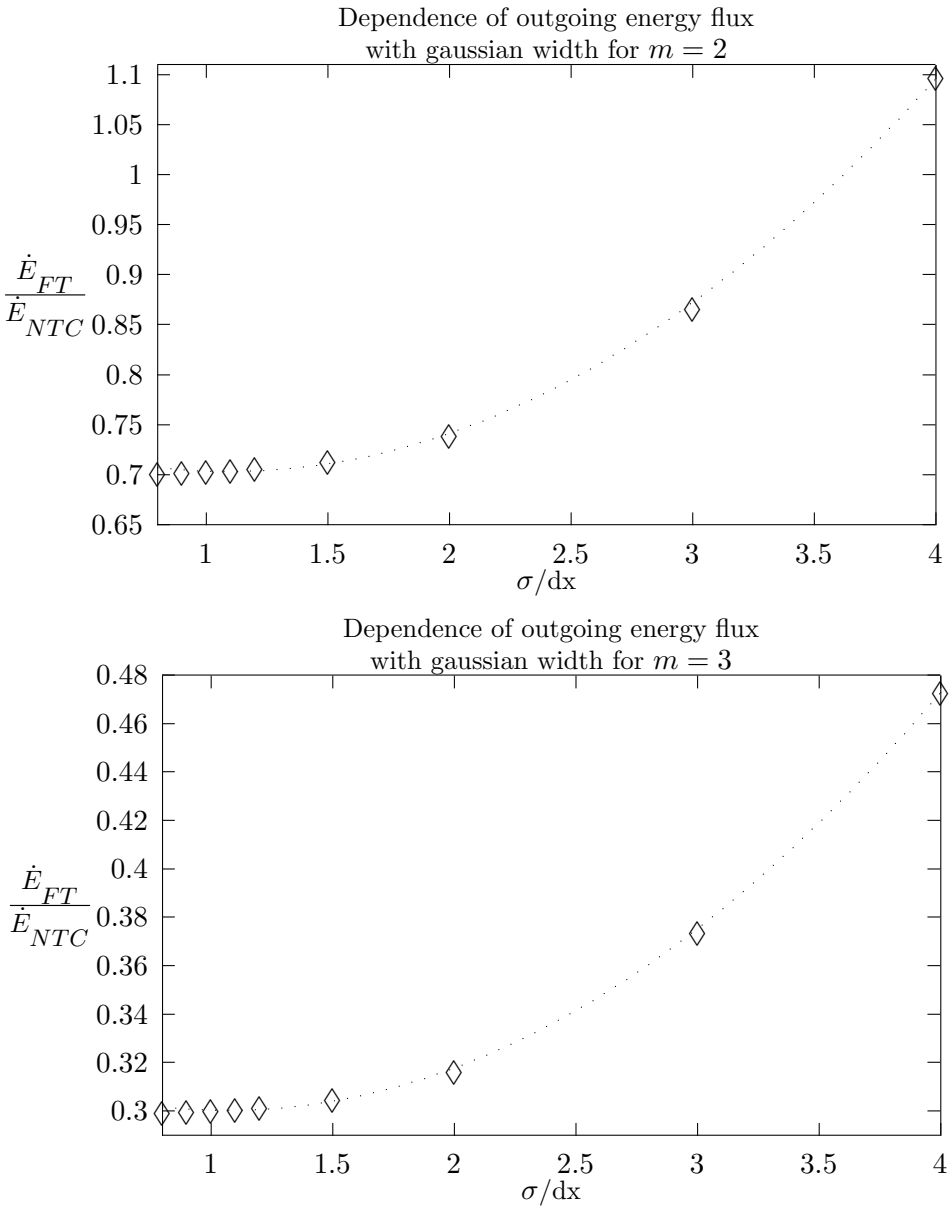

Fig. 5.1. Convergence of the gaussian approximation. Plotted here is the ratio of the high precision results of Ref. [18] (denoted here as $\dot{E}_{FT}$) and the average energy flux radiated for a circular equatorial orbit around a Schwarzschild hole ($\dot{E}_{NTC}$) as a function of the relative gaussian width used in our method of evolving the Teukolsky equation in the time domain. This is for a sample case consisting of a circular orbit around a hole of $a = 0.9$ at $r = 5\, r_{isco}$.

$$\Psi_{(h)} = \Psi_{exact} + Ch^{a} + \mathbf{O}(h^{a+1}) \tag{5.1}$$

Therefore, if we run at various resolutions we can get a quantity $\mathcal{C}$ that measures the order of convergence a of the code. This is defined as

$$\mathcal{C} = \left\| \frac{\Psi_{(4h)} - \Psi_{(2h)}}{\Psi_{(2h)} - \Psi_{(h)}} \right\|_2 \tag{5.2}$$

In Figure 5.2 we show for a representative run simulating a particle of $\mu = 0.005M$ on a circular equatorial orbit at $r = 7M$ and for the multipole $m = 2$, how the 2-norm of the quantity $\mathcal{C}$ shows second order convergence of the algorithm.

5.3 Gravitational Energy Flux and Teukolsky waveforms

In this section we show representative results for the evolution of the Teukolsky waves and the energy flux measured far from the black hole for various representative cases of circular orbits around various values for the black hole spin a, the inclination angle of the orbit ι, and the orbital radii r. Animated versions of these and similar evolutions will be available on the Web version of this dissertation[28].

These results aim to show what particle orbit perturbative evolutions look like, and more importantly to demonstrate in practice the capabilities of the method and are not meant to match or surpass the accuracy of similar studies done in the frequency domain. In the next chapter, we will discuss how this numerical framework for analysis of non-homogeneous black hole perturbative evolutions can be used and what technical

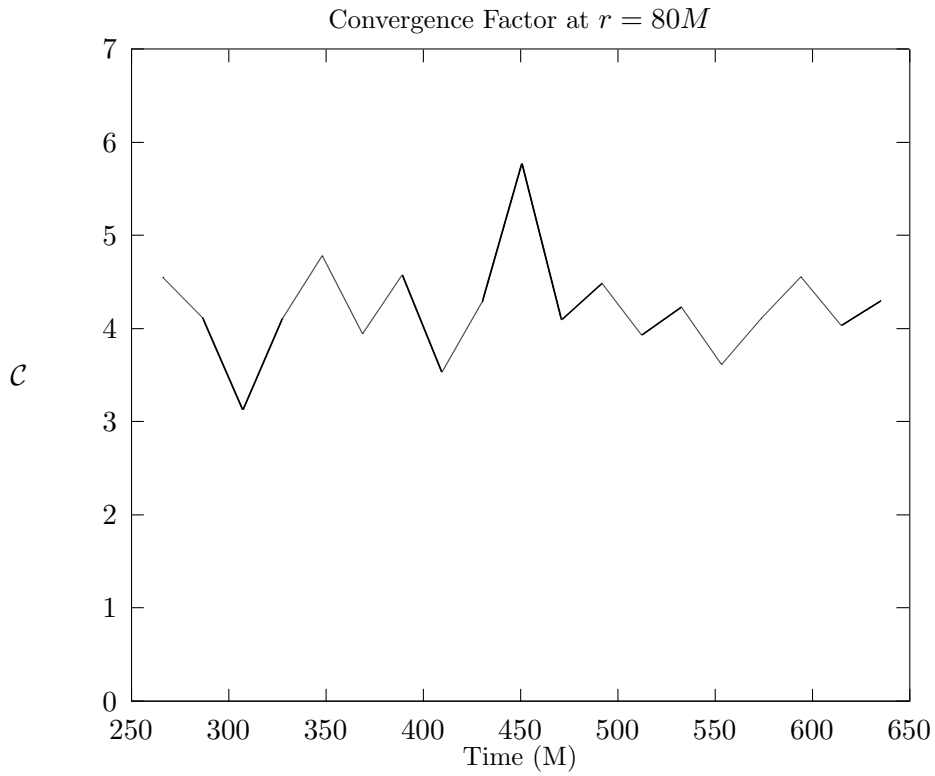

Fig. 5.2. 2-norm of the convergence ratio $\mathcal{C}$ of Eq. (5.2) calculated for $\mathbf{Re}[\Psi]$ at a Boyer-Lindquist radial distance of $r = 80M$ for three simulations with radial resolutions of 2000, 4000 and 8000 gridpoints.

details need to be solved and/or improved to achieve comparable accuracies in those future results.

5.3.1 Equatorial orbits

The following figures show the real and imaginary parts of the Teukolsky function Φ at various times in the orbit of radius $r = 5\, r_{isco}$ for a representative value of $m = 2$. This is for a particle of $\mu = 0.01M$ around a black hole of spin $a = 0.9$.

The next set figures show the real and imaginary parts of the Teukolsky function Φ at various times for another type of equatorial orbit. This time one of radius $r = 3\,r_{isco}$ for a representative value of $m = 2$. This is for a particle of $\mu = 0.01M$ around a black hole of spin $a = 0.5$.

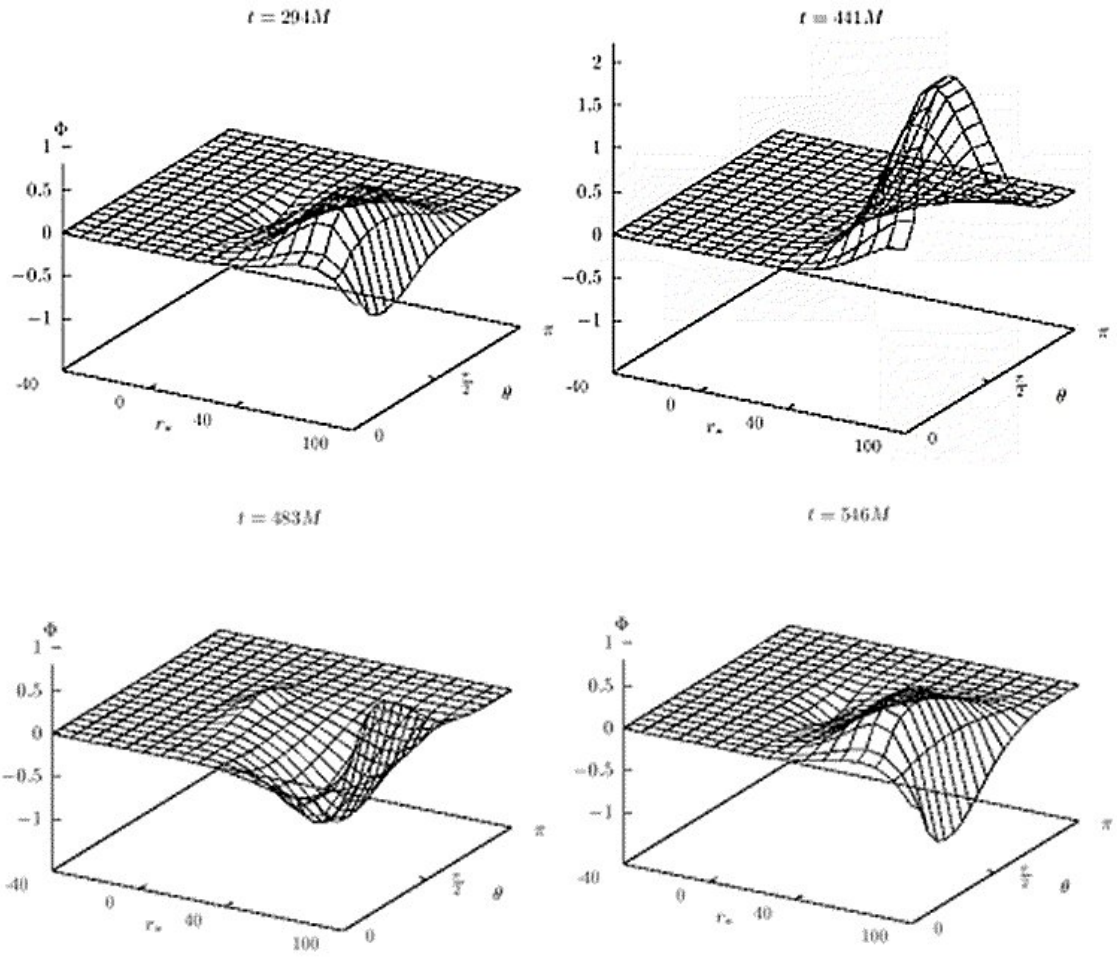

Fig. 5.3. The real part of the numerical Teukolsky function Φ for the $m = 2$ mode of an equatorial orbit of radius $r = 5\,r_{isco}$ at different times. The particle parameters are $\mu = 0.01M$ around a black hole of spin $a = 0.9$.

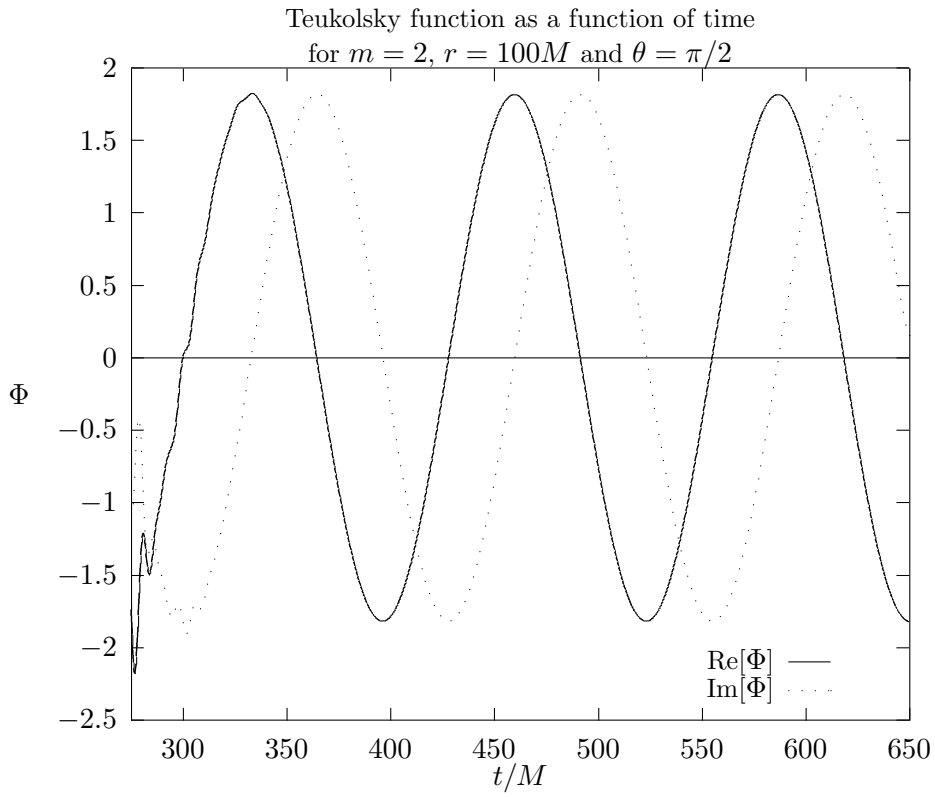

Fig. 5.4. This figure shows the value of the function Φ as a function of Boyer-Lindquist time at a distance of $r = 100M$ and in the equatorial plane of the black hole for the same parameters of Fig. 5.3.

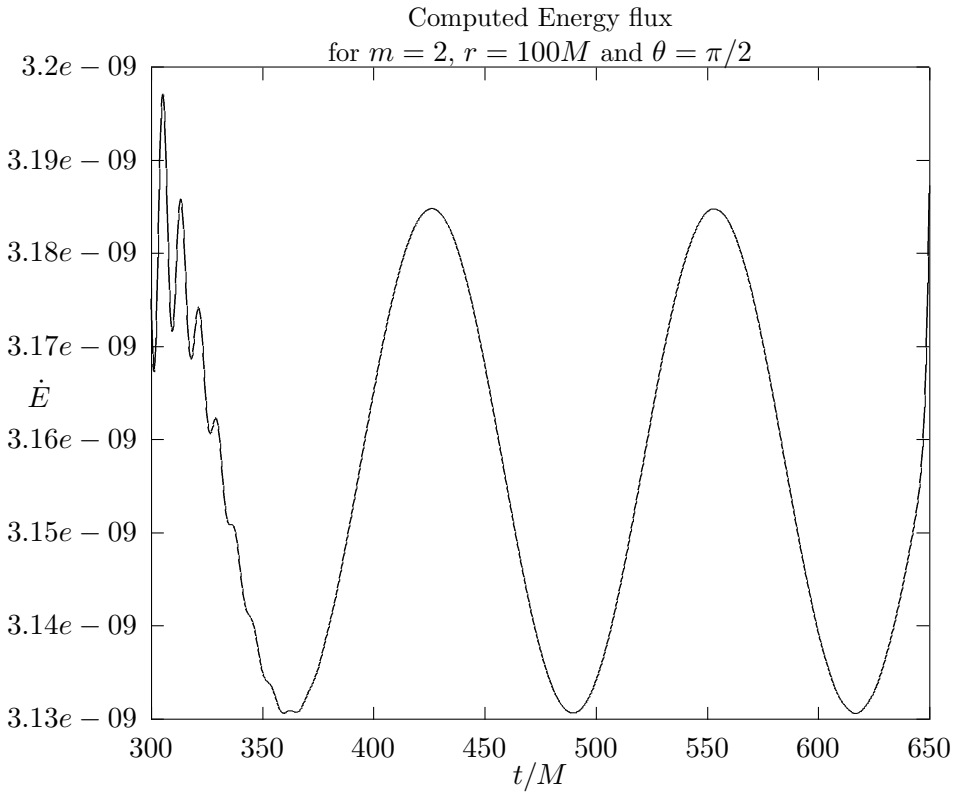

Fig. 5.5. Energy flux measured in the equatorial plane at a distance of $100M$ from the horizon for the same case of the two preceding figures.

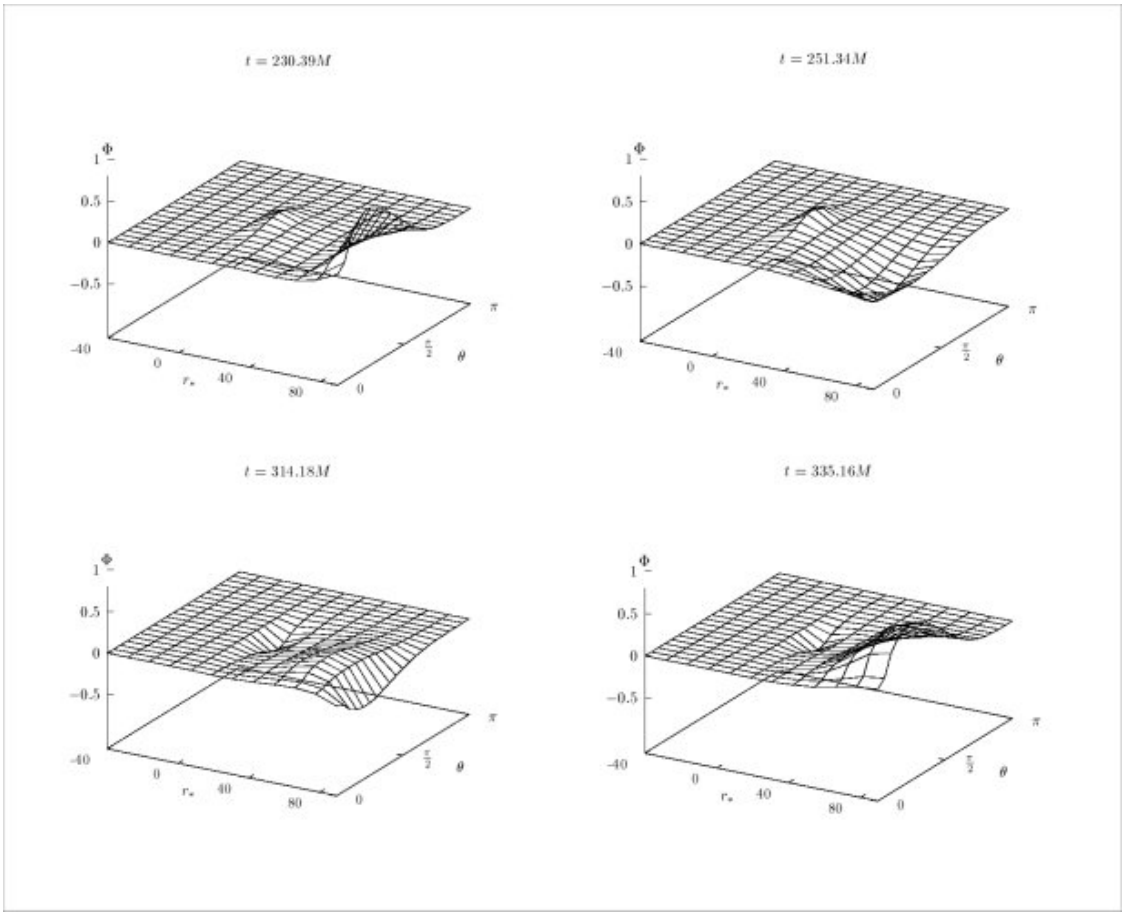

Fig. 5.6. The real part of the numerical Teukolsky function Φ for the $m = 2$ mode of an equatorial orbit of radius $r = 3\,r_{isco}$ at different times. The particle parameters are $\mu = 0.01M$ around a black hole of spin $a = 0.5$.

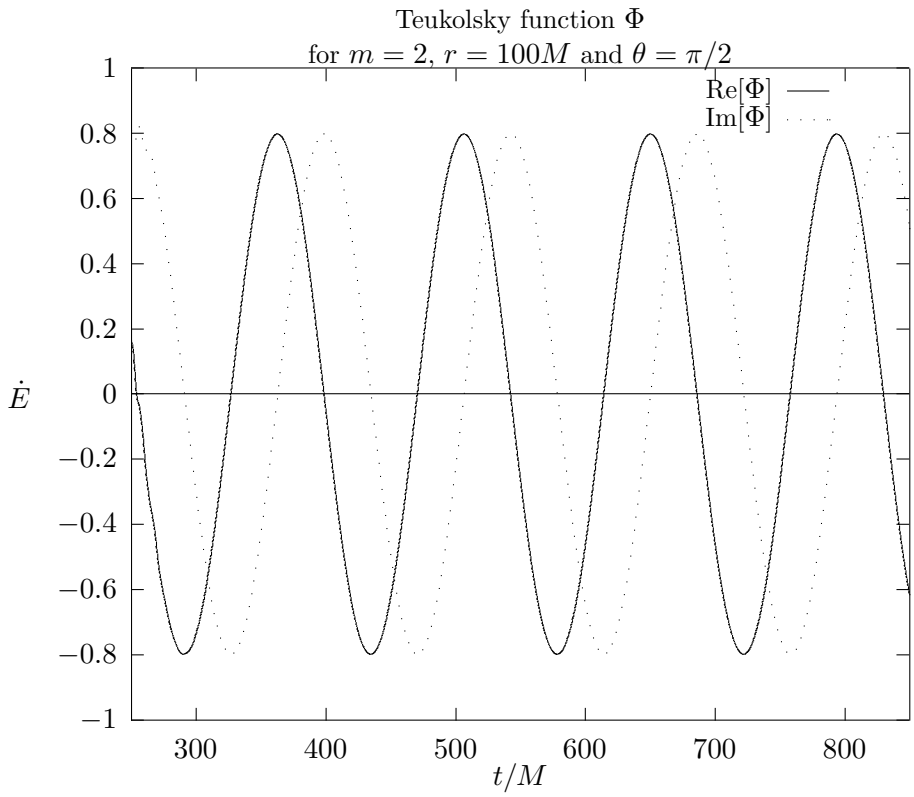

Fig. 5.7. This figure shows the value of the function Φ as a function of Boyer-Lindquist time for $m = 2$ at a distance of $r = 100M$ and in the equatorial plane of the black hole for the same parameters as in Fig. 5.6.

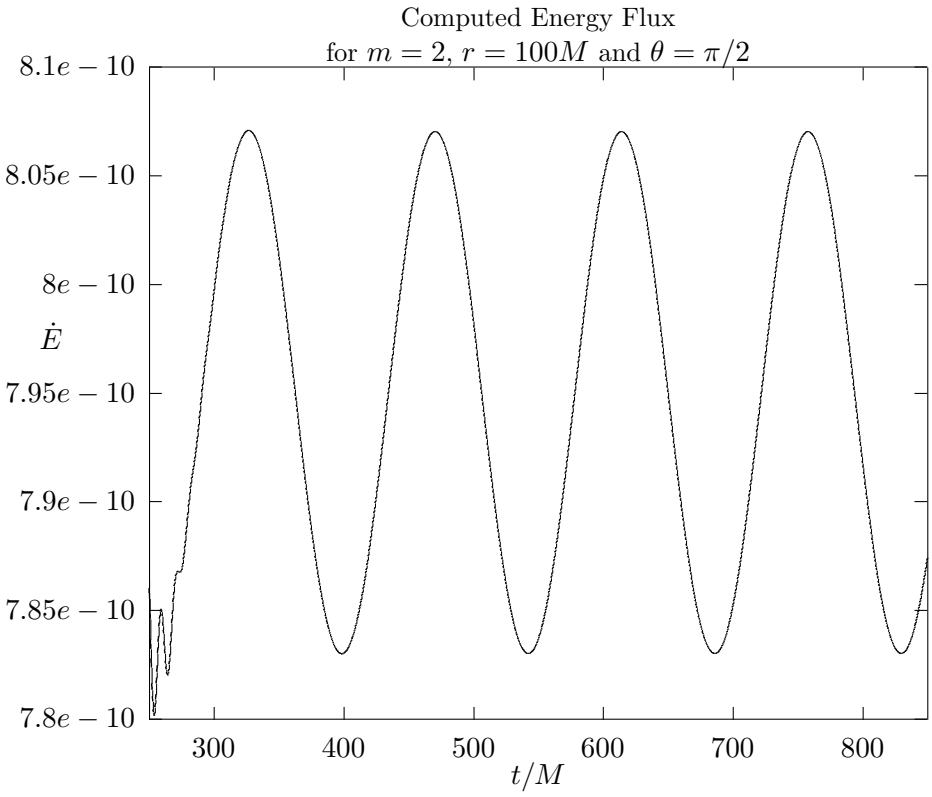

Fig. 5.8. Energy flux measured at a distance of $100M$ from the horizon for the mode $m = 2$ for the same case of the two preceding figures.

5.3.2 Inclined orbits

Circular orbits that do not lie on the equatorial plane of a Kerr hole have only been done very recently by Hughes[19] using the "circular-to-circular" radiation reaction that forms the basis of our present analysis and that we discussed extensively on the last chapter. Here we present Teukolsky waveforms and energy flux graphs that were produced by our code and a graph illustrating the wave amplitude that would be seen by LISA from such an orbit.

For the representative orbital decay shown here we used a starting point of orbital radius $r = 7M$, black hole spin $a = 0.95M$ and angle of inclination $\iota = 62.43^{\circ}$. The procedure followed the discussion already given in Section 4.3. Specifically, we do a circular orbit by specifying a circular geodesic trajectory for the peak of the gaussian mass distribution that simulates the particle and evolving for 4-10 orbits at a radial resolution of 6000 points and an angular resolution of 20 points. We output tables of the Teukolsky function Φ, the energy flux, and the angular momentum flux of the outgoing wave at a distance of $100M$ at every 600 timesteps (corresponding to a time interval of $20.5M$). Each table has the value of those quantities at radial intervals of $8.2M$ and at each angular gridpoint.

We average the energy and angular momentum fluxes for the whole orbits that occur in the time window defined after the spurious burst that occurs due to the unphysical choice of initial data has passed and before some of it has bounced off the outer edge of the grid and comes back to the point where this quantity is "measured". The changes in the energy, angular momentum, Carter constant and inclination angle of the orbit

are calculated by multiplying those $\langle \frac{dE}{dt} \rangle$ and $\langle \frac{dJ}{dt} \rangle$ by the time required to complete 5-10 full orbits at that radius and using Eqs. 4.15, 4.16, and 4.20. We change the input parameter set $\{r, L_z, E, Q, \theta_{max}\}$ by those amounts and that defines the next circular orbit in the decay sequence that we are studying. In Figure 5.9 we depict the evolution of the Teukolsky function for 5 of those decay sequences by pasting together the data that the program outputs in each of those separate runs.

Because we closely followed Hughes' method of emulating radiation reaction, and we tested our code's handling of inclined orbits with one of the cases he treated in the frequency domain, we saw fit to include here three graphs from Ref. [19]. They are meant to illustrate the way in which inclination angles change due to radiation reaction, and the gravitational wave signal that would be seen by LISA for our fiducial starting $r = 7M$ and $\iota = 62.43^{\circ}$ inclined orbit written in the conventional $h_{\times}$ and h_{+} amplitude form.

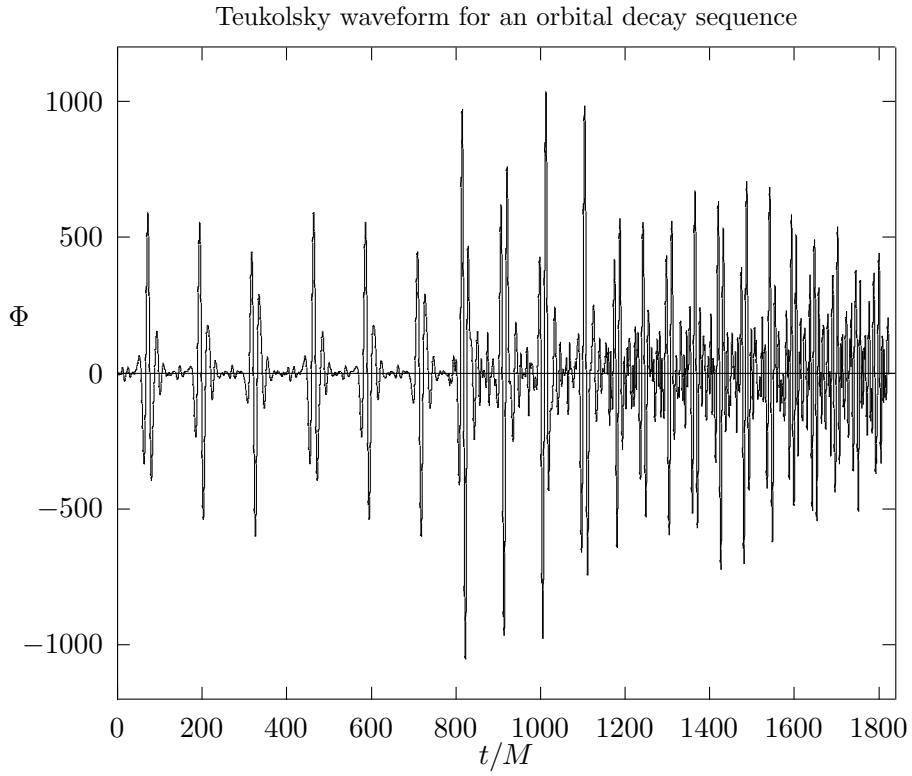

Fig. 5.9. The real part of the numerical Teukolsky function Φ as a function of time for a sequence of circular orbits starting at $r = 7M$, $a = 0.95$ and $\iota = 62.43^{\circ}$ for a particle of $\mu = 0.001$ connected together by radiation reaction.

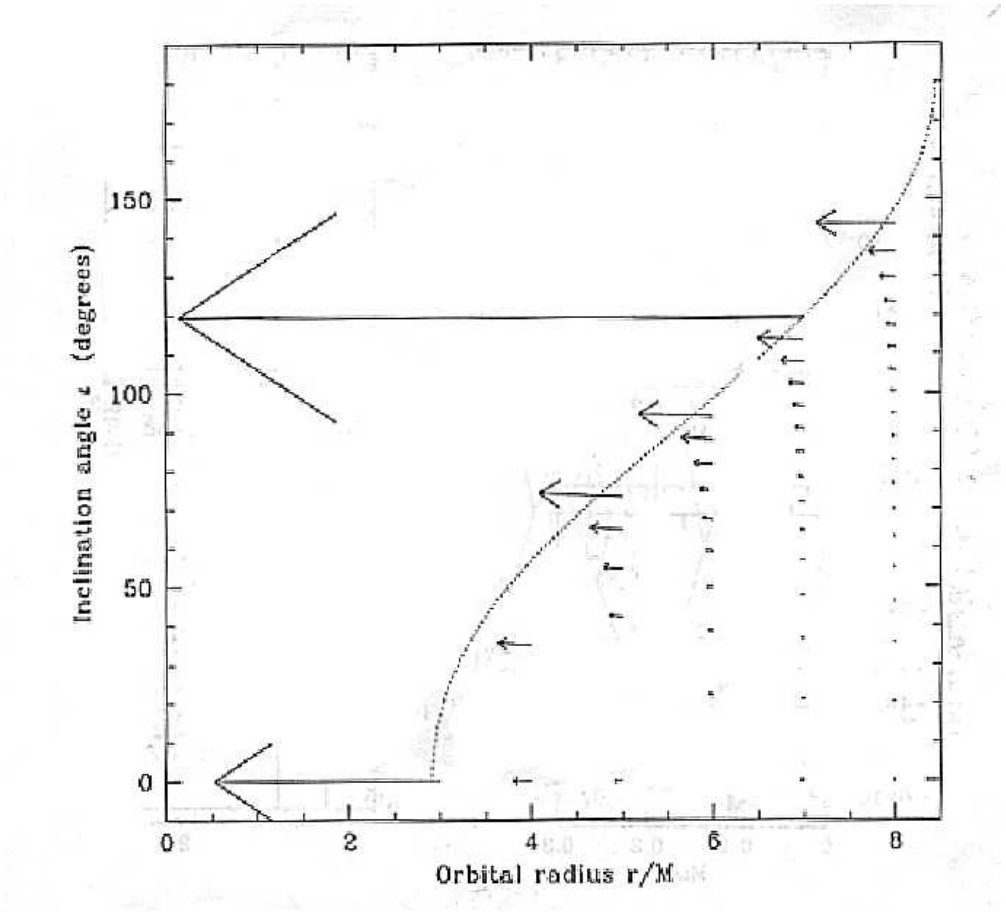

Fig. 5.10. Effects of radiation reaction for a black hole of $a = 0.8$. The dotted line is the maximum allowed inclination angle; any orbit beyond that line will be unstable and plunge into the hole. Each arrow is proportional to the vector $[(M/\mu)\dot{r}, (M/\mu)\dot{\iota}]$. The arrow indicates the direction in phase space in which the orbit will move after radiation reaction.

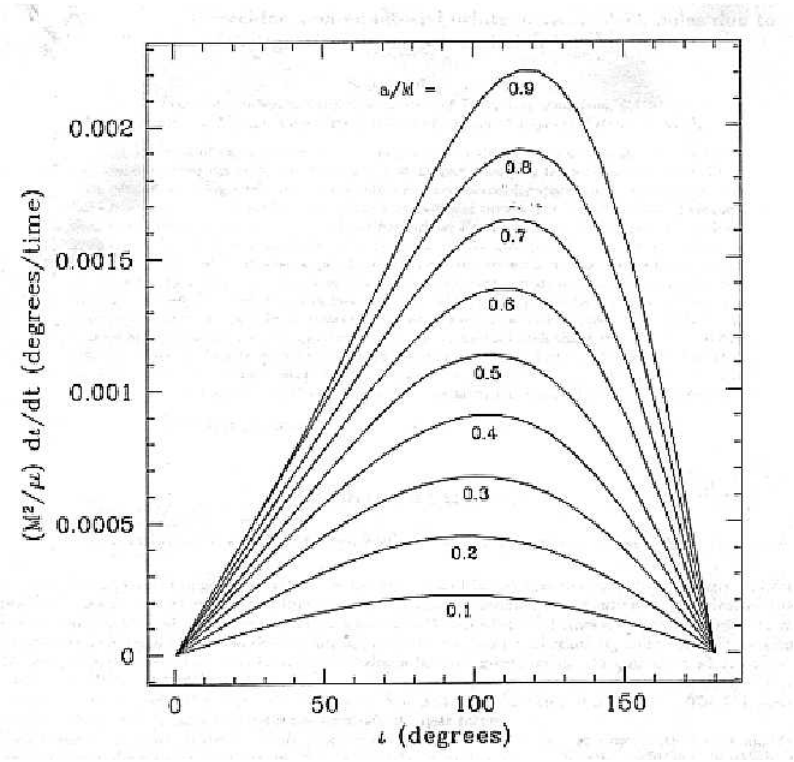

Fig. 5.11. The rate of change of the orbit inclination (i) as a function of the initial inclination angle for various values of the central black hole spin a. All curves are for a circular orbit of radius $r = 10M$.

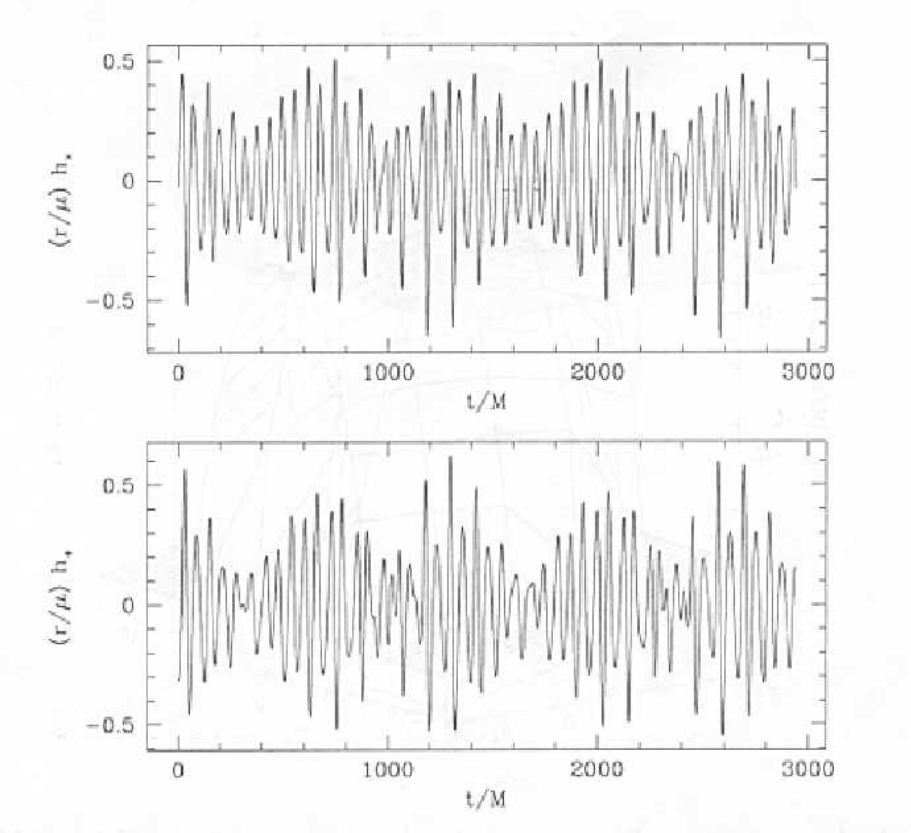

Fig. 5.12. Gravitational waveforms for the case treated here of $r = 7M$ and $\iota = 62.43^{\circ}$ about a black hole of $a = 0.95M$. These are seen at the equatorial plane of the hole. One can see many prominent and sharp features indicating the strong contribution of many harmonics of the fundamental frequencies Ω_{θ} and Ω_{φ}.

Chapter 6

Conclusions

6.1 Particle motion around supermassive black holes and future LISA observations

The particle limit is a very important clue for unraveling the two-body problem in General Relativity and for providing valuable insights for attacking the "holy grail" of Numerical Relativity, the theoretical solution of a general asymmetric binary black hole collision. Perturbative analysis of astrophysically realistic particle orbits have been impossible so far because there is no computationally useful prescription for calculating $\dot{Q}$, and this is absolutely necessary for modeling the motion of the particle in the strong field region near the horizon where Post-Newtonian methods may not be reliable and where for rapidly rotating central holes the particle may linger for thousands of orbits, and where the bulk of the detectable useful signal is expected to be.

LISA is expected to fly in a decade or so, and joint discussions currently underway between NASA and ESA give hope to many relativists that the prospects for the mission are quite optimistic. Then, the problem of theoretically modeling inclined elliptic particle orbits around supermassive holes takes a note of increased urgency since the data is building up indicating that such huge $10^6 - 10^8 M_\odot$ are common in the center of Active Galactic Nuclei (AGNs) at least. Finn and Thorne [18] have published a paper analyzing the likelihood and frequency distribution of such extreme mass-ratio binary systems and

how their signal-to-noise ratios would make them ideal candidates for easy detection with LISA. They base their analysis on the output calculated for circular equatorial orbits and the outlook looks quite good and makes one hopeful that more general orbits will produce easily waves on a regular basis with a much richer structure and with lots of interesting information about the strong-field region of the black hole encoded in their signal.

The final pieces needed for completing a theoretical model of general particle orbits would be to fully develop a computationally viable prescription for calculating local radiation reaction forces and using that information to move form one orbit to next as long as the particle moves under conditions in which the adabiatic approximation is valid. Also one needs to model the rapid plunge of the particle into the black hole once the ISCO is crossed, and it would be nice to do that in a perturbative fashion.

There has been considerable advances along those lines of research. We discussed in detail in Section 4.4 how recent proposals have been proposed to understand how geodesic orbits change due to the local self-force of the field of the particle to first order. To incorporate radiation reaction in a numerical simulation of matter around black holes would seem to require the use of time-domain methods to evolve perturbations as the path of the particle changes more and more rapidly as it enters the strong-field region near the horizon, or at the very least that would seem to be the more natural way to proceed at this stage.

Progress in the "plunge" of the problem has been achieved recently by using the "close-limit" approximation[3]. Baker *et al* have used full numerical relativity in the very beginning of a set of runs with various members of a set whose initial data for

equal-mass black holes have increasing values for the linear momenta and start very near the ISCO and testing when the evolution can be switched with confidence to a perturbative treatment and obtain plausible plunge waveforms. They also study how the linearization time (the time where one can switch from full numerical evolutions to the close-limit treatment with confidence) varies with the holes of the momentum.

More applicable to our method is a work done by Ori and Thorne[36] in which they derive an expression for the equation of motion of a particle in a circular equatorial orbit in the "transition regime" very near the ISCO where the orbit goes from that of adiabatically slow changes from one circular orbit to the next to the more rapid and essentially geodesic plunge into the hole. They rewrite the geodesic equation for radial motion in terms of an effective potential that basically depends on the radial distance of the particle and on the difference $\xi \equiv \tilde{L} - \tilde{L}_{isco}$ of its dimensionless orbital angular momentum from that of the ISCO. By calculating how the location of the minimum of this effective potential changes as ξ decreases after the emission of radiation they can write an equation of motion for this transition regime which looks like

$$\frac{d^2X}{dT^2} = -X^2 - T \tag{6.1}$$

where the quantities X and T are defined in terms of the radial difference $R \equiv \tilde{r} - \tilde{r}_{isco}$ and the normalized proper time $\tilde{\tau}$ as

$$X = \frac{R}{\eta^{2/5} R_{o}} \, , \quad T = \frac{\tilde{\tau} \eta^{1/5}}{\tau_{o}} \, ; \tag{6.2}$$

$$R_{o} = (\beta\kappa)^{2/5} \alpha^{-3/5} \, , \quad \tau_{o} = (\alpha\beta\kappa)^{-1/5} \, ; \tag{6.3}$$

$$\alpha = \frac{1}{4} \left(\frac{\partial^3 V(\tilde{r}, \tilde{E}, \tilde{L})}{\partial \tilde{r}^3} \right)_{\rm isco} \, , \tag{6.4}$$

$$\beta = -\frac{1}{2} \left(\frac{\partial^2 V(\tilde{r}, \tilde{E}, \tilde{L})}{\partial \tilde{L} \partial \tilde{r}} + \tilde{\Omega} \frac{\partial^2 V(\tilde{r}, \tilde{E}, \tilde{L})}{\partial \tilde{E} \partial \tilde{r}} \right)_{\rm isco} \, . \tag{6.5}$$

$$\kappa = \frac{32}{5} \tilde{\Omega}_{\rm isco}^{7/3} \frac{1 + a/\tilde{r}_{\rm isco}^{3/2}}{\sqrt{1 - 3/\tilde{r}_{\rm isco} + 2a/\tilde{r}_{\rm isco}^{3/2}}} \dot{\mathcal{E}}_{\rm isco} \, ; \tag{6.6}$$

We did not use this equation of motion in this work because it is only applicable to circular equatorial orbits, but it certainly seems feasible to extend the idea of writing an effective potential for the 2-D geodesic motion of the r and θ coordinate directions and to get similar equations of motion for the transition regime of inclined circular orbits at least. This would be relatively easy to incorporate in our code as it would only need to switch from the subroutine which now calculates the position of the particle using the geodesic equations (4.6) - (4.9) to one written to update the position using the effective equation of motion in the transition regime. This way one could in principle follow a particle in the strong-field region from the outer adiabatic regime to the ISCO to the plunge and get accurate gravitational waveforms at infinity.

6.2 Directions of future research

There remains some more work to be done in this time-domain approach to evolving matter source motion around rotating black holes using this approximation of substituting narrow gaussian distributions for the location of the particles in the computational grid. To get comparable accuracies to those achieved on frequency domain calculations such as Post-Newtonian methods or the Teukolsky-Sasaki-Nakamura formulation we need to deal with the following technical issues:

(a) correctly rewriting the Teukolsky potential of Eq. (2.39) because for high values of m the potential grows too rapidly near $\theta \sim 0$ and in the region of the maximum of $\frac{\partial \tilde{V}}{\partial r}$ this produces exponentially growing spikes that contaminate the waves in the interior rapidly and eventually crash the code. To get better accuracies we need much more values of m that the ones we are presently using.

(b) the choice of initial data. We have a simple but unphysical choice of initial data which makes the particle appear out of nowhere and therefore producing a huge burst of "junk" radiation that we basically ignore by letting it pass thru the point where we are going to monitor the correct evolution of the system and discarding that data and looking only at the waves produced by the stable particle orbits. To get many orbits and to get good averages not only in time but also in various spatial directions we need to define a very large grid that is there mostly to have this burst proceed unmolested without "bouncing" on the outer boundaries of the domain or else the boundary reflections from the burst would contaminate the waveforms coming from the particle orbits. Getting better initial data in the spirit of those proposed in Ref. [29] may help in reducing this

initial burst and therefore having the bulk of the computational resources being more efficiently used in the region where the waves are generated and/or monitored.

The main conclusion of this research is that the method appears feasible, and it looks like there are no unsurmountable problems in its basic conception and implementation. One is optimistic that it can be successfully adapted to help in the problem of implementing numerical simulations in which radiation reaction is taken into account, even for general elliptical orbits around rapidly rotating holes.

Other ideas that could be explored with the use of this numerical code in the near future include:

1. Update the equation of motion to include the effects of spinning test particles. The basic equations of motion of a spinning test particles in curved spacetimes have been formulated by Papapetrou and Dixon [17, 38]. Suzuki and Maeda [55] have studied the effects of a non-zero spin tensor in the stability of circular orbits around Kerr black holes and how the location of the ISCO is affected by the spin of the particle. By modifying the geodesic equations of motion, we could include spin effects to get more realistic waveform evolutions.

2. Study in more detail how practical it would be to attempt to write routines that will approximate the "tail-term" integrations in equations of motion like those of Quinn and Wald [45] and how to get estimates for $\dot{Q}$ from the comparison of purely geodesic orbits and those that could be evolved from these type of prescriptions. It would be very interesting to see what kinds of accuracy one could get with such approximations.

3. If the above ideas result practical, one could tackle the problem of extending the analysis of Finn and Thorne [18] to catalog relativistic corrections to quadrupole radiation formulae, study how long will waveforms last before the particle S/N ratio falls below the noise curve for LISA, and estimate what kinds of frequency bandwidths will those inclined systems sweep through in the last year before the hole captures the compact object.

We have described in detail our research in constructing the matter source term for a particle moving in the in the strong field region of a Kerr black hole. This was done using a previously successful approximation for locating the point particle in the discrete grid of a numerical simulation by substituting the delta function that describes its location in the source term by a narrow gaussian distribution whose derivatives can still be resolved at the resolution of the grid used in the program. The methodology seems consistent and with a suitable extrapolation procedure can reproduce adequately earlier results for treatable orbits done in the frequency domain, bolstering our confidence in the results obtained at this stage. If some technical issues that hamper the algorithm's accuracy can be resolved successfully, the code seems to be ideally suited to tackle the still unsolvable problem of modeling inclined elliptical orbits all the way to the innermost stable orbit and beyond. In principle, it could also be used to study the effects of accretion disks for gravitational wave sources by coupling it to fully relativistic hydrodynamics using the Smoothed Particle Hydrodynamics (SPH) routines that have been previously used in the **CGPG** group [27].

References

[1] T. Apostolatos, D. Kennefick, A. Ori, and E. Poisson. *Phys. Rev. D*, 47:5376, 1993.

[2] R. Arnowitt, S. Deser, and C.W. Misner. *Gravitation:An Introduction to Current Research*. John Wiley, NY, 1962. edited by L. Witten.

[3] J. Baker, B. Brugmann, M. Campanelli, C.O. Lousto, and R. Takahashi. *gr-qc/0102037*, 2001. (submitted for publication in Phys. Rev. D).

[4] J.M. Bardeen and W.H. Press. *J. Math. Phys.*, 14:7, 1973.

[5] J. Bowen and J. York. *Phys. Rev. D*, 21:2047, 1980.

[6] R.H. Boyer and R.W. Lindquist. *J. Math. Phys.*, 8:265, 1975.

[7] R.A. Breuer. *Gravitational Perturbation Theory and Synchrotron Radiation*, volume 44 of *Lecture Notes in Physics*. Springer-Verlag, 1975.

[8] M. Campanelli and C.O. Lousto. *Phys. Rev. D*, 59:124022, 1999.

[9] M. Campanelli, C.O. Lousto, J.Baker, G. Khanna, and J. Pullin. *Phys. Rev. D*, 58:084019, 1998.

[10] S. Chandrasekhar. *The Mathematical Theory of Black Holes*. Oxford University Press, NY, 1983.

[11] C. Cutler, L.S. Finn, E. Poisson, and G.J. Sussman. *Phys. Rev. D*, 47:1511, 1993.

[12] C. Cutler, D. Kennefick, and E. Poisson. *Phys. Rev. D*, 50:3816, 1994.

[13] M. Davis, R. Ruffini, W.H. Press, and R.H. Price. *Phys. Rev. Lett.*, 27:21, 1971.

[14] S.L. Detweiler. *Astrophys. J.*, 225:687, 1978.

[15] S.L. Detweiler and E. Szedenits. *Astrophys. J.*, 231:211, 1979.

[16] B.S. DeWitt and R.W. Brehme. *Ann. Phys. (N.Y.)*, 9:220, 1960.

[17] W.G. Dixon. *Philos. Trans. R. Soc. London*, A277:59, 1974.

[18] L.S. Finn and K.S. Thorne. *Phys. Rev. D*, 62:124021, 2000.

[19] S.A. Hughes. *Phys. Rev. D*, 61:084004, 2000.

[20] D. Kennefick and A. Ori. *Phys. Rev. D*, 53:4319, 1996.

[21] R.P. Kerr. *Phys. Rev. Lett.*, 11:237, 1963.

[22] G. Khanna, R. Gleiser, R. Price, and J. Pullin. *New Journal of Phys.*, 2:3.1–3.17, 2000. (http://www.njp.org).

[23] W. Kinnersley. *J. Math. Phys.*, 10:1195, 1969.

[24] Y. Kojima and T. Nakamura. *Phys. Lett.*, 96A:335, 1983.

[25] Y. Kojima and T. Nakamura. *Prog Theor Phys*, 71:79, 1984.

[26] W. Krivan, P. Laguna, P. Papadopoulos, and N. Andersson. *Phys. Rev. D*, 56:3395, 1997.

[27] P. Laguna, W.A. Miller, and W.H. Zurek. *Astrophys. J.*, 404(1):678, 1993.

[28] R. Lopez-Aleman. *Evolving Particle Trajectories Perturbatively Around Rotating Black Holes in the Time Domain*. PhD thesis, Penn State University, 2001. (http://www.phys.psu.edu/ lopez/Thesis/index.html).

[29] C.O. Lousto and R.H. Price. *Phys. Rev. D*, 56:6439, 1997.

[30] C.O. Lousto and R.H. Price. *Phys. Rev.D*, 55:2124, 1997.

[31] Y. Mino, M. Sasaki, M. Shibata, H. Tagoshi, and T. Tanaka. *Prog. Theor. Phys. Suppl.*, 128:121, 1997.

[32] Y. Mino, M. Sasaki, and T. Tanaka. *Phys. Rev. D*, 55:3457, 1997.

[33] V. Moncrief. *Ann. Phys. (NY)*, 88:323, 1974.

[34] R. Narayan. *Astrophys. J.*, 536:663, 2000.

[35] E.T. Newman and R. Penrose. *J. Math. Phys.*, 6:918, 1962.

[36] A. Ori and K.S. Thorne. *Phys. Rev. D*, 62:124022, 2000.

[37] P. Papadopoulos and J.A. Font. *Phys. Rev.D*, 59:044014, 1999.

[38] A. Papapetrou. *Proc. R. Soc. London*, A209:248, 1951.

[39] E. Poisson. *Phys. Rev. D*, 47:1497, 1993.

[40] E. Poisson. *Phys. Rev. D*, 48:1860, 1993.

[41] E. Poisson. *Phys. Rev. D*, 52:5719, 1995.

[42] E. Poisson and M. Sasaki. *Phys. Rev. D*, 51:5753, 1995.

[43] W.H. Press, S.A. Teukolsky, W.T. Vetterling, and B.P. Flannery. *Numerical Recipes in FORTRAN*. Cambridge University Press, 2 edition, 1992.

[44] R.H. Price and J. Pullin. *Phys. Rev. Lett.*, 72:3297, 1994.

[45] T.C. Quinn and R.W. Wald. *Phys. Rev. D*, 56(6):3381, 1997.

[46] T.C. Quinn and R.W. Wald. *Phys. Rev. D*, 60:064009, 1999.

[47] T. Regge and J.A. Wheeler. *Phys. Rev.*, 108:1063, 1957.

[48] R.Geroch, A. Held, and R. Penrose. *J. Math. Phys.*, 14:874, 1973.

[49] R. Ruffini. *Phys. Rev.D*, 7:972, 1973.

[50] J. Ruoff, P. Laguna, and J. Pullin. *gr-qc/0005002*, 2000.

[51] F. D. Ryan. *Phys. Rev. D*, 53:3064, 1996.

[52] M. Sasaki and T. Nakamura. *Prog Theor Phys*, 96A:1788, 1982.

[53] M. Shibata, M. Sasaki, H. Tagoshi, and T. Tanaka. *Phys. Rev. D*, 51:1646, 1995.

[54] S. Sigurdsson and M.J. Rees. *Mon. Not. R. Astron. Soc.*, 284:318, 1997.

[55] S.Suzuki and K. Maeda. *Phys. Rev. D*, 58:023005, 1998.

[56] J. Stewart and M. Walker. *Black Holes: The outside story*, volume 69 of *Springer Tracts in Modern Physics*. Springer-Verlag, 1973.

[57] T. Tanaka, M. Shibata, M. Sasaki, and T. Nakamura. *Prog. Theor. Phys.*, 90:65, 1993.

[58] S.A. Teukolsky. *Astrophys. J.*, 185:635, 1973.

[59] R.M. Wald. *General Relativity.* Univ Of Chicago Press, 1984.

[60] F.J. Zerilli. *Phys. Rev. Lett.*, 24:737, 1970.

Vita

Ramon Lopez-Aleman was born in Bayamon, Puerto Rico in September 3, 1961. He got his B.S. degree in Physics from the University of Puerto Rico in 1983. He also earned a Masters degree in Electrical Engineering from Cleveland State University in 1986. He worked as a Research Assistant at the Standard Oil of Ohio Research Labs in Warrensville, OH in 1984-85; and at the Laser Spectroscopy Laboratory of the Physics Department of the University of Puerto Rico in 1993-95. He was a Physics Instructor at the InterAmerican University of Puerto Rico from 1986-1987. He is a professor at the Physical Sciences Dept. of the University of Puerto Rico, Rio Piedras since 1987. He was Department Chairman from 1994 to 1995.

Ramon Lopez-Aleman is a member of the American Physical Society and the American Association of Physics Teachers.